UNIVERSIDADE FEDERAL DE SANTA CATARINA
CAMPUS TRINDADE OU CENTRO TECNÓLOGICO
PROGRAMA DE PÓS-GRADUAÇÃO EM ENGENHARIA QUÍMICA

Luis Eduardo Castro Anaya

Intermolecular potential optimization for enhancing CO2 olubility predictions in tertiary amine based solvents

Florianópolis, SC
2023

Luis Eduardo Castro Anaya

Intermolecular potential optimization for enhancing CO2 olubility predictions in tertiary amine based solvents

Dissertação submetida ao Programa de Pós-Graduação em Engenharia Química da Universidade Federal de Santa Catarina para a obtenção do título de mestre em Engenharia Química.
Advisor: Prof. Dr. Sergio Yesid Gómez González
Co-advisor: Prof. Dr. Gustavo Adolfo Orozco Alvarado

Florianópolis, SC
2023

Ficha de identificação da obra elaborada pelo autor,
através do Programa de Geração Automática da Biblioteca Universitária da UFSC.

Castro Anaya, Luis Eduardo
Intermolecular potential optimization for enhancing CO2 solubility predictions in tertiary amine based solvents / Luis Eduardo Castro Anaya ; orientador, Sergio Yesid Gómez González, coorientador, Gustavo Adolfo Orozco Alvarado, 2023.
69 p.

Dissertação (mestrado) - Universidade Federal de Santa Catarina, Centro Tecnológico, Programa de Pós-Graduação em Engenharia Química, Florianópolis, 2023.

Inclui referências.

1. Engenharia Química. 2. CO2 capture. 3. Molecular Dynamics. 4. Tertiary amine and alkanolamine. 5. Physical Solubility. I. Gómez González, Sergio Yesid. II. Orozco Alvarado, Gustavo Adolfo. III. Universidade Federal de Santa Catarina. Programa de Pós-Graduação em Engenharia Química. IV. Título.

Luis Eduardo Castro Anaya

Intermolecular potential optimization for enhancing CO2 olubility predictions in tertiary amine based solvents

O presente trabalho em nível de mestrado foi avaliado e aprovado por banca examinadora composta pelos seguintes membros:

Prof. Dr. Sergio Yesid Gómez González
Universidade Federal de Santa Catarina - PosENQ

Prof. Dr. José Vladimir de Oliveira
Universidade Federal de Santa Catarina - PosENQ

Prof.(a) Dr. Giovanni Finoto Caramori
Universidade Federal de Santa Catarina - PPGQ

Certificamos que esta é a **versão original e final** do trabalho de conclusão que foi julgado adequado para obtenção do título de mestre em Engenharia Química.

Documento assinado digitalmente
Debora de Oliveira
Data: 13/12/2023 18:12:13-0300
CPF: ***.453.929-**
Verifique as assinaturas em https://v.ufsc.br

Coordenação do Programa de
Pós-Graduação

Documento assinado digitalmente
Sergio Yesid Gomez Gonzalez
Data: 13/12/2023 18:07:57-0300
CPF: ***.911.889-**
Verifique as assinaturas em https://v.ufsc.br

Prof. Dr. Sergio Yesid Gómez González
Advisor

Florianópolis, SC, 2023.

This work is dedicated to my beloved grandparents:
Judith, Lucila, Plutarco and Luis.

ACKNOWLEDGEMENTS

To my mother, my father and my sister, who always took care of me, supported me in my decisions and without whom none of this would be possible.

To my uncles and aunt, for always showing me their support and listening, especially to my uncle Javier, who was always aware of my progress and who is always a source of inspiration and calm.

To those people who are my other family, who through conversations, laughter, experiences, but above all their unique way of being gave me the emotional support necessary to carry out this work: Thanks to Diana, Valentina, Paulo, Patrick, Juan David and David.

Thanks to Professor Gustavo for the trust, teachings and opportunities provided and especially for always encouraging me to pursue goals to the best of my abilities.

Thanks to Professor Sergio for his guidance beyond academic, experiential, and who always encouraged me to value my efforts.

Thanks to the Foundation for the Improvement of Higher Education Personnel (CAPES) and to Brazil in general for providing the material support for my stay in Brazil and for carrying out this research.

I thank all the people who in one way or another were part of this journey.

Thanks again to all of them.

Finally, thanks to God.

RESUMO

A captura de dióxido de carbono (CO2) é um componente crucial para mitigar as emissões de gases de efeito estufa e enfrentar as mudanças climáticas. Soluções de aminas terciárias e alcanoaminas têm mostrado promessa como absorventes eficientes de CO2 devido à sua alta capacidade de absorção, estabilidade química superior e custos energéticos mais baixos em comparação com aminas primárias e secundárias. Compreender e ser capaz de prever a solubilidade do CO2 nessas soluções, quantificada pela constante da Lei de Henry (HLC), é fundamental para projetar e otimizar o processo de captura. O principal objetivo desta dissertação foi aprimorar a precisão e o poder preditivo dos cálculos de HLC em aminas terciárias. Isso foi alcançado por meio da otimização de um modelo de potencial intermolecular, que serve de base para os cálculos de HLC. Foi estabelecido um arcabouço teórico sobre a solubilidade física e química do dióxido de carbono em aminas terciárias, bem como uma revisão da literatura dos dados experimentais disponíveis para esses solventes puros e dos estudos computacionais relevantes sobre o cálculo dessa propriedade. No curso deste trabalho, utilizamos o campo de força AUA4 para a representação das moléculas orgânicas, para o qual foi implementado no software de simulação molecular GROMACS e validado para a recriação computacional efetiva das propriedades de equilíbrio das substâncias puras. Juntamente com o modelo ZHU para o dióxido de carbono, eles formam o alvo de otimização do potencial intermolecular. Foi desenvolvida uma abordagem inovadora para otimizar o modelo de potencial intermolecular para interações CO2-amina, empregando propriedades em excesso de misturas binárias supercríticas específicas recriadas com simulações de dinâmica molecular para otimizar eficientemente todos os parâmetros LJ para a interação entre os átomos de oxigênio do dióxido de carbono (O(CO2)) e os carbonos terminais (CH3), carbonos secundários (CH2) e átomos de oxigênio do grupo hidroxila (O(H)). O modelo de potencial otimizado foi validado e empregado para calcular os valores de HLC para hexano, etanol, 4-metilmorfolina, trietilamina, metil dietanolamina e trietanolamina, e comparado com dados experimentais criticamente revisados. A precisão na previsão das propriedades de equilíbrio e a eficiência computacional dos modelos moleculares usados no potencial intermolecular foram garantidas e mostraram ser superiores ou iguais a outros modelos moleculares de detalhe físico semelhante. O potencial intermolecular otimizado melhorou geralmente a precisão das previsões de HLC para o CO2, reduzindo a discrepância de 22,2% para 10,0% e garantindo o comportamento correto dessa propriedade com a temperatura. Embora seja necessária uma otimização e validação com uma quantidade maior de dados experimentais, este modelo fornece resultados qualitativamente consistentes com os dados experimentais e se destaca como um dos primeiros modelos moleculares otimizados e avaliados no estudo do CO2 nesta classe de solventes. Esta dissertação contribuiu para o campo da captura de dióxido de carbono, aprimorando nossa capacidade de prever as constantes da Lei de Henry em álcoois e aminas terciárias e alcanoaminas. O modelo de potencial intermolecular otimizado oferece uma ferramenta valiosa para pesquisadores e engenheiros envolvidos no desenvolvimento de tecnologias de captura de carbono, possibilitando soluções mais eficientes e sustentáveis para a mitigação das emissões de CO2.

Palavras-chave: Captura de dióxido de carbono. Amina terciária. Alcanolaminas. Simulações de Dinâmica Molecular. Constante de Henry (HLC). Potencial otimizado.

ABSTRACT

Carbon dioxide (CO2) capture is a crucial component of mitigating greenhouse gas emissions and addressing climate change. Tertiary amine and alkanolamines solutions have shown promise as efficient CO2 absorbents due to its high absorption capacity, superior chemical stability and lower energy costs compared to primary and secondary amine. Understanding and being able to predict the solubility of CO2 in these solutions, as quantified by Henry's law constant (HLC), is paramount for designing and optimizing the capture process. The primary objective of this dissertation was to enhance the accuracy and predictive power of HLC calculations in tertiary amine. This was achieved through the optimization of an intermolecular potential model, which forms the basis for HLC computations. A theoretical framework concerning the physical and chemical solubility of carbon dioxide in tertiary amines was established, as well as a literature review of the experimental data available for these pure solvents and the relevant computational studies on the calculation of this property. In the course of this work, we employed the AUA4 force field for the representation of the organic molecules, for which it was implemented in the free molecular simulation software GROMACS and validated for the computationally effective recreation of the equilibrium properties of the pure substances. Together with the ZHU model for carbon dioxide they form the intermolecular potential optimization target. A novel approach to optimize the intermolecular potential model for CO2-amine interactions was developed, employing excess properties form specific binary supercritical mixtures recreated with molecular dynamics simulations to efficiently optimize the every LJ parameters for the interaction between oxygen atoms of the carbon dioxide (O(CO2)) and the terminal carbon (CH3), the secondary carbon (CH2) and oxygen of the hydroxyl group (O(H)) sites. The optimized potential model was validated and employed to calculate HLC values for Hexane, ethanol, 4-methylmorpholine, Triethylamine, Methyl diethanol amine and Triethanolamine and compared with critically reviewed experimental data. The accuracy in predicting the equilibrium properties and computational efficiency of the molecular models used in the intermolecular potential was guaranteed and shown to be superior or equal to other molecular models of similar physical detail. The optimized intermolecular potential generally improved the accuracy of HLC predictions for CO2, by reducing the deviation from 22.2% to 10.0% and ensuring the correct behavior of this property with temperature. Although an optimization and validation with a larger amount of experimental data must be further performed, this model provides qualitatively consistent results with the experimental data and stands out as one of the first molecular models optimized and evaluated in the study of CO2 in this class of solvents. This dissertation has contributed to the field of carbon dioxide capture by enhancing our ability to predict Henry's law constants in alcohols and tertiary amines and alkanolamines. The optimized intermolecular potential model offers a valuable tool for researchers and engineers involved in the development of carbon capture technologies, enabling more efficient and sustainable solutions for mitigating CO2 emissions.

Keywords: Carbon dioxide capture. Tertiary amine. Alkanolamines. Molecular Dynamic Simulations. Henry's law constant (HLC). Optimized potential.

RESUMO EXPANDIDO

Introdução A captura de CO2 é uma medida necessária para reduzir as emissões de gases de efeito estufa e combater as mudanças climáticas. Entre as tecnologias disponíveis, a captura com solventes físicos e químicos se destaca como a alternativa mais madura e de aplicação mais fácil. A eficácia dessa alternativa depende em grande parte da escolha do solvente e de suas propriedades físicas. Nesse sentido, soluções de aminas terciárias e alcanoaminas são absorventes promissores de CO2, pois têm alta capacidade de absorção, estabilidade química superior e custos energéticos mais baixos do que soluções de aminas primárias e secundárias. Compreender e prever a solubilidade física do CO2 nesses tipos de solventes, conforme medida pela constante da lei de Henry (HLC), é fundamental para o projeto e otimização do processo de captura, pois essa propriedade desempenha um papel fundamental na modelagem cinética e de transferência de massa e, por fim, na viabilidade do processo de absorção de CO2. Nesse sentido, a química computacional e, em particular, as simulações moleculares são particularmente úteis, pois são capazes de capturar interações moleculares e chegar a previsões significativamente precisas da HLC. No entanto, poucos estudos computacionais foram realizados sobre a solubilidade do dióxido de carbono em alcanoaminas, e os estudos sobre aminas terciárias são limitados e não verificam a reprodução correta da solubilidade física do dióxido de carbono nessa classe de solventes. Alguns desses estudos destacaram a necessidade de ajustar as interações moleculares entre o dióxido de carbono e as moléculas do solvente, o que apresenta um desafio adicional, já que o cálculo da HLC por simulações moleculares é intensivo em termos computacionais. Portanto, este trabalho encurta a lacuna entre modelos moleculares, conhecidos como campos de força, e previsões precisas e economicamente viáveis da solubilidade física, implementando, validando e otimizando o potencial intermolecular entre o CO2 e os grupos moleculares do solvente. Para isso, propusemos (1) coletar e analisar dados experimentais disponíveis para aminas terciárias e alcanoaminas terciárias à luz da abordagem termodinâmica da Lei de Henry (2) implementar e avaliar um campo de força capaz de recriar com custos computacionais reduzidos as propriedades de equilíbrio dos solventes (3) otimizar as interações intermoleculares cruzadas entre o solvente e o dióxido de carbono usando dados de excesso disponíveis e (4) avaliar a capacidade do potencial intermolecular de reproduzir a solubilidade física do dióxido de carbono em aminas terciárias e alcanoaminas terciárias.

Metodologia Para o desenvolvimento do trabalho, utilizamos o software gratuito GROMACS para simular a dinâmica molecular. O campo de força AUA4 foi usado para representar as moléculas de substâncias orgânicas, enquanto o modelo ZHU foi utilizado para o dióxido de carbono. O campo de força AUA4 foi avaliado para a reprodução das propriedades de equilíbrio ao simular a interface vapor-líquido por meio de uma caixa retangular. A partir disso, por meio de ajustes tangenciais e análises de teste de pressão, foram obtidas a densidade do líquido, a densidade do vapor e a pressão de saturação. Posteriormente, tanto as fases líquida quanto de vapor foram simuladas, e as entalpias de cada fase e, finalmente, a entalpia de vaporização foram obtidas. Por outro lado, um esquema sequencial de otimização das interações cruzadas entre os átomos de oxigênio do dióxido de carbono e os sítios atômicos correspondentes ao carbono terminal (CH3), ao carbono secundário (CH2) e ao oxigênio do grupo hidroxila

(O(H)) foi planejado. A otimização desses grupos foi realizada por minimização sequencial do desvio quadrático na previsão do volume molar em excesso e da entalpia em excesso de cada mistura binária de CO2 com etano, hexano e etanol. O cálculo das propriedades em excesso foi realizado com base nos resultados das simulações de dinâmica molecular em condições supercríticas em quatro composições diferentes. O modelo otimizado foi avaliado na reprodução da constante de Henry, que foi calculada por meio de simulações de energia livre de Gibbs usando a metodologia da Razão de Aceitação de Bennett. Para isso, foram realizadas 20 simulações com 20 fatores de acoplamento igualmente espaçados para inserir uma molécula de CO2 em uma caixa com 1000 moléculas de solvente. Esses resultados foram comparados com dados experimentais de solubilidade física de CO2 que foram coletados e analisados criticamente à luz da abordagem da lei de Henry.

Resultados Na avaliação do campo de força AUA4, foi observado um alto nível de concordância na reprodução das propriedades de equilíbrio, com desvios de aproximadamente 2,13% para densidade, 4,91% para entalpia de vaporização e 8,30% para pressão de vapor. O campo de força AUA4 se destaca pelo seu erro muito baixo no cálculo da entalpia de vaporização em comparação com outros modelos (OPLS-AA, GAFF e CGenFF), o que indica uma boa representação da energia interna das moléculas estudadas, exceto para o ácido acético. Em relação à densidade, o campo de força AUA4 tem um bom desempenho, ficando logo atrás do campo de força TraPPE-UA. Em termos de desempenho computacional, o uso do campo de força AUA4 em comparação com um campo de força All-atoms mostrou um ganho computacional de duas vezes a velocidade. O processo de otimização foi bem-sucedido em esclarecer a reprodução das propriedades em excesso, sendo a modificação mais significativa a interação entre o carbono terminal e o oxigênio do dióxido de carbono, que não excede 5%. A magnitude dessas mudanças corresponde bem aos resultados obtidos em outros estudos, nos quais a otimização dos parâmetros de interação intermolecular levou a modificações de até +15%. Por outro lado, a interação com o oxigênio do grupo hidroxila necessitou de poucos ajustes. A avaliação do modelo otimizado mostrou melhora nas previsões de solubilidade em hexano, reduzindo o erro médio de 33,6% para 11,2%. Uma melhoria significativa é observada nas previsões de solubilidade em etanol, reduzindo o desvio de um desvio médio absoluto de 23,2% para 3,5%. Isso destaca a alta sensibilidade da HLC a esses parâmetros e valida o procedimento de otimização. Além disso, o potencial otimizado pode ser extrapolado (transferido) até temperaturas tão altas quanto 373,15 K. Nas aminas terciárias, TRE e NMM, o desvio foi reduzido de +28,5% para +11,2% e aumentou de +3,7% para -14,1%, respectivamente. Isso se explica pelo fato de que a interação com a amina terciária não foi otimizada. Finalmente, a aplicação do potencial para a reprodução da HLC em alcanoaminas terciárias mostra concordância entre os dados experimentais em altas temperaturas, enquanto em baixas temperaturas não pode ser determinada porque os dados experimentais provavelmente estão sendo mascarados pela solubilidade química do dióxido de carbono.

Conclusão A principal conclusão deste trabalho é que um potencial intermolecular otimizado por propriedades em excesso, com a capacidade de melhorar a previsão

da solubilidade do dióxido de carbono em alcanoaminas, foi alcançado com sucesso. Algumas informações importantes a esse respeito são: (1) Existem possíveis reações químicas nos dados de solubilidade de aminas terciárias, e a extensão da reação parece diminuir com a temperatura, mascarando a solubilidade física em até quatro vezes. Essa distinção entre solubilidade física e química é um passo essencial para a seleção dos dados experimentais usados na avaliação do potencial intermolecular otimizado. (2) O modelo AUA4 foi implementado e validado com sucesso para o estudo das propriedades de equilíbrio de substâncias orgânicas, com precisão igual ou superior à de outros modelos de detalhes físicos semelhantes e provou fornecer eficiência computacional duas vezes superior à dos modelos "all-atom". (3) Foi demonstrada a capacidade de usar dados de entalpia em excesso e volume em excesso para melhorar a previsão da solubilidade física. Um conjunto de 6 parâmetros de interação intermolecular correspondentes aos valores sigma e epsilon dos sítios atômicos que formam qualquer álcool linear: álcoois e alcanos lineares, pôde ser otimizado de forma econômica por meio de um esquema de otimização sequencial. As correções encontradas foram menores ou iguais às de trabalhos semelhantes que realizam a otimização desses parâmetros moleculares diretamente na constante da lei de Henry. O ajuste mais significativo ocorreu na interação entre o carbono terminal e os átomos de oxigênio do dióxido de carbono. (4) O potencial intermolecular otimizado melhorou significativamente as previsões da constante de Henry nas moléculas usadas no processo de otimização. Também garantiu que o comportamento com a temperatura fosse corretamente reproduzido mesmo em temperaturas mais altas do que as contempladas no processo de otimização. O potencial intermolecular otimizado também mostrou sinais de melhoria na previsão da solubilidade em aminas terciárias, no caso de TRE, reduziu o desvio de 24%AAD para pouco mais de 11%AAD. No geral, houve uma redução do erro de 22,3%AAD para 10,0%AAD. (4) As previsões do potencial intermolecular otimizado nas alcanoaminas terciárias, como MDEA, mostraram que, em altas temperaturas, há uma correspondência entre os dados previstos pelo modelo e os dados experimentais, enquanto em baixas temperaturas há dados experimentais insuficientes e os que existem provavelmente são influenciados pela solubilidade química do CO2.

LIST OF FIGURES

LIST OF TABLES

LIST OF ABBREVIATIONS AND ACRONYMS

AA	All-Atoms
AAD	Absolute Average Deviation
CAS	Chemical Abstract Service Registry Number
CCSU	Carbon capture, storage, and utilization
CHARMM	Chemistry at Harvard Macromolecular Mechanics Force Field
CO2	Carbon Dioxide
DEA	Diethanolamine
DMEA	Dimethyl ethanolamine
EtOH	Ethanol
GAFF	General AMBER Force Field
GROMOS	GROningen MOlecular Simulation Force Field
HEX	Hexane
IPCC	Intergovernmental Panel on Climate Change
MDEA	Methyl diethanolamine
MEA	Monoethanolamine
N2O	Nitrous Oxide
NMM	4-Methylmorpholine
NMR	Nuclear Magnetic Resonance
NPT	Isobaric-isotermic ensemble
NVT	Isocoric-isotermic ensemble - canonical ensemble
OPLS	Optimized Potential for Liquid Simulations
QSPR	Quantitative Structure Property Relationship
RMSD	Root Mean Square Deviation
TEA	Triethanolamine
TraPPE	Transferable Potential for Phase Equilibria
TRE	Triethylamine
UA	United-Atoms

LIST OF SYMBOLS

U_{total}	Total potential energy
U_{intra}	Intramolecular potential energy
U_{inter}	Intermolecular potential energy
σ	Distance parameter of Lennard-Jones potenttial
ε	Energy parameter of Lennard-Jones potenttial
q_i	Electric charge over particle i
k_{bend}	Bond-bending force constant
θ	Angle formed between two adjacent bonds
φ	Dihedral angle
ρ	Mass density
h	Enthalpy
P	Pressure
V	Volume
x_i	Mole fracction of component i
μ	Chemcial potential
H	Henry law constant
R	Gas constant
T	Temperature

CONTENTS

1 INTRODUCTION

Global warming, resulting from the excessive release of greenhouse gasses, has become one of the most pressing challenges facing our planet today. Among these gasses, carbon dioxide (CO2) is a significant contributor to the greenhouse effect, driving climate change and its associated impacts on the environment and human society. To mitigate this issue, the Intergovernmental Panel on Climate Change (IPCC) pointed out carbon capture, storage, and utilization (CCSU) as a necessary mitigation measure to achieve scenarios of constant reduction of carbon dioxide emissions that ultimately lead to a limit warning amount by the end of the 21st century (SHUKLA et al., 2022). This scenario shows the need to shift from a fossil to a renewable energy framework, making CCSU the first energy security scheme, and an unavoidable action for thriving in the future (MADEJSKI et al., 2022).

The first stage of CCSU involves the separation of carbon dioxide from the process streams of chemical industries or power plants. The technologies available for this stage can be classified according to the separation mechanism as is shown in Figure 1:

Figure 1 – Carbon capture technologies.

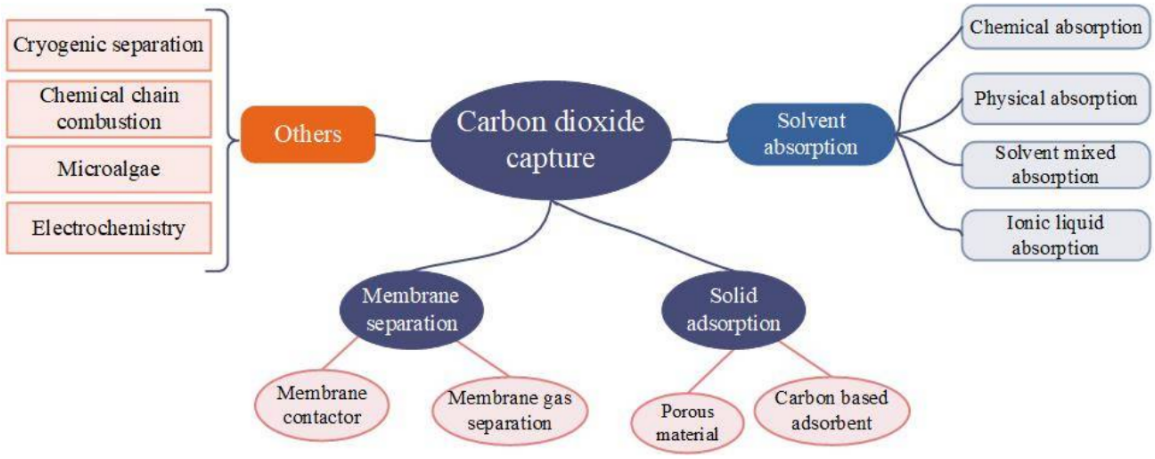

Source: Taken from (LIU, E.; LU; WANG, D., 2023)

In particular, solvent absorption is the most mature technology, inherited from natural gas sweetening processes, in which acid gasses such as carbon dioxide and hydrogen sulfide are separated from a high-pressure stream containing mainly methane. Some authors have classified solvent-based absorption technologies based on the presence or absence of chemical reactions, thereby discerning whether the absorption process is primarily chemical or physical. This categorization stems from the intrinsic characteristics of the solvents used, with solvent types containing amine groups, such

as amines, alkanolamines, and nucleic acids, regarded as chemical solvents. Typical examples of these kind of solvents are monoethanolamine, diethanol amine and methyl diethanol amine and piperazine. In contrast, solvents like ethers, alcohols, and glycols are considered physical solvents. Some well-established solvents retrieving from natural gas sweetening process are Rectisol (methanol), Fluor (Propylene Carbonate), and Selexol (Dimethyl Ether of Polyethylene Glycols).

However, it is essential to note that chemical solvents also exhibit physical solubility phenomena, commonly expressed by the Henry law constant. This property holds significant interest as it serves as a cornerstone in the kinetic and mass transfer modeling in chemical absorption solvents while simultaneously being the primary focus in physical absorption solvents.

The benchmark case of chemical absorption is the use of a 30% by weight solution of monoethanolamine (MEA), a primary amine known for its relatively rapid reaction for carbamate formation and low viscosity (DUTCHER; FAN; RUSSELL, 2015). However, this compound presents problems of corrosion, degradation, relatively high volatility, and a high energetic penalty for the regeneration of the solvent, which is related to the high stability of the carbamate. In contrast, tertiary amines have a lower absorption rate but have a higher carbon dioxide absorption capacity, are less corrosive, and generally have a lower regeneration energy (N.BORHANI; WANG, M., 2019). Therefore, the study and selection of this type of amines and blends of these amines with other solvents to improve their properties are emerging research topics in carbon dioxide capture (CHOWDHURY et al., 2013; LIU, S. et al., 2019; WANDERLEY; PINTO; KNUUTILA, 2021).

It is crucial to develop accurate models and predictions of physicochemical properties to make significant advancements in selecting optimal solvents and their mixtures. Additionally, experimentation is an uphill task, and the chemical spectrum of possible solvents is immense (PAPADOPOULOS; ZAROGIANNIS; SEFERLIS, 2017). These models must capture the molecular interactions between the CO2 and the solvent molecules to aid in identifying the optimal conditions for enhanced CO2 solubility, leading to more efficient discovery and enhancement of carbon capture processes, reducing the time and effort of prospecting solvents using in silico approaches.

In recent years, computational chemistry and molecular simulations have witnessed remarkable progress, allowing for exploring intermolecular interactions at the atomic level. Such advancements have empowered researchers to test and tune intermolecular potentials, offering valuable insights into the behavior of in mixtures of water (OROZCO; ECONOMOU; PANAGIOTOPOULOS, 2014), alcohols (AIDA et al., 2010) and primary amines (OROZCO; LACHET; MACKIE, 2016). However, computational chemistry studies focused on tertiary amines are limited and and need to be more accurate in verifying the correct reproduction of the physical solubility of carbon dioxide

in this class of solvents.

Additionally, in the quest to broaden our understanding of gas solubility in tertiary amines and related solvents, it becomes evident that the trade-off between computational demand and result accuracy becomes a central concern. The ability to predict gas solubility in such systems with precision relies heavily on the choice of molecular models. Therefore, cost-effective, highly accurate molecular models are paramount. Striking the right balance between computational efficiency and result accuracy is crucial for advancing our understanding of gas solubility and ensuring the practical applicability of these simulations in various scientific and industrial contexts.

The primary objective of this dissertation is to bridge the gap between molecular models, more precisely referred to as force fields, and accurate physical solubility predictions by optimizing the intermolecular potential between CO2 and solvent molecular groups. By doing so, we aim to enhance the understanding of the molecular-level interactions that govern CO2 physical absorption and, consequently, contribute to developing a more efficient selection of solvents for carbon capture applications and better kinetic and mass transfer modelings.

This research will employ state-of-the-art molecular dynamic techniques, such as molecular dynamics simulations for free energy calculations, and ultimately, the computation of Henry's law constant. The accuracy and reliability of the optimized intermolecular potential were ensured by capturing a comprehensive set of data and validating the results against available experimental observations.

Accurate predictions of CO2 solubility in tertiary amines and alkanolamines can also find applications in other fields, such as gas separation processes, solvent design, and the development of green chemistry practices. Hence, the potential impact of this research extends beyond carbon capture technologies alone.

1.1 OBJECTIVES

1.1.1 General Objective

Develop an optimized intermolecular potential targeting higher cost-efficient computational calculations of the physical solubility of carbon dioxide in tertiary amines and tertiary alkanolamines by refining the intermolecular cross-interaction parameters.

1.1.2 Specific Objectives

a) To analyze existing experimental data to identify and differentiate the chemical and physical solubility of CO2 in tertiary amines and alkanolamines.

b) To implement and assess a transferable, accurate, and inexpensive molecular model suitable for studying the equilibrium properties of functional groups involved in tertiary amines and alkanolamines.

c) To optimize the intermolecular cross-interactions between solvent atom sites and carbon dioxide sites from excess property data.

d) To assess the intermolecular potential's ability to reproduce carbon dioxide's physical solubility in tertiary amines and alkanolamines with state-of-the-art molecular dynamic methods.

1.2 RESEARCH IMPACT

The novelty and potential impact of the herein research led to the conception of two scientific papers. The first corresponds to the previously presented second objective. The article, titled "Comprehensive Automated Routine Implementation, Validation, and Benchmark of the Anisotropic Force Field (AUA4) Using Python and GROMACS", was recently published in the Journal of Physical Chemistry A (DOI: doi.org/10.1021/acs.jpca.2c08335). A direct product of this paper is an automated Python routine for creating simulation files necessary for the simulation of the molecular model used in this research. Although this routine is mentioned in this work, all the details of its implementation and validation are not shown here but can be reviewed directly in the paper. The second article, oriented by the third and fourth objectives, is still under development.

2 THEORICAL FRAMEWORK

This section describes the thermodynamic principles of carbon dioxide's physical and chemical absorption, reviewing studies on tertiary amines as solvents for carbon dioxide capture and the characteristics of using solutions of these compounds as solvents. Additionally, the concepts of force field, intermolecular potential, and molecular dynamics are briefly discussed to review the computational studies related to solubility prediction and its relevance in carbon dioxide capture technologies. Finally, the available experimental data on this property in tertiary amines are presented.

2.1 PHYSICAL AND CHEMICAL SOLUBILITY OF CO2

The physical solubility of gasses into liquids is commonly described by the Henry law, which states that at infinite dilution, the composition of the solute is linearly related to its partial pressure Equation (1) (PRAUSNITZS; LICHTENTHALER; GOMES DE AZEVEDO, n.d.). In this way, higher values of the Henry constant are related to less solute in the solvent and, ultimately, with less solubility. Therefore, this physicochemical property reflects the interaction between the solvent and the gas molecules. Henry constant is a strong function of temperature while the pressure effect is corrected by the Poynting factor, as is shown in equation (2). Changes in this property with temperature and pressure are the principle behind carbon dioxide separation using physical solvents; these are solvents that do not interact chemically with carbon dioxide, only physically (SMITH, K. H. et al., 2022).

$$f_i = P \cdot y_i \cdot \varphi_i = H_{i,solvent} \cdot x_i \tag{1}$$

$$ln\left(\frac{f_i}{x_i}\right) = ln\left(H_{i,solvent}\right) + \frac{\overline{v}_i^{\infty} \cdot \left(P - P_{solvent}^{(sat)}\right)}{RT} \tag{2}$$

In aqueous solutions, Carbon dioxide acts as a volatile, weak electrolyte, meaning that the molecule of CO2 establishes a gas-liquid equilibrium and a chemical equilibrium in solution (EDWARDS et al., 1978). The solvated carbon dioxide ($CO_{2(ac)}$) reacts with water to form the carbonic acid ($H_2CO_{3(ac)}$) as it is expressed in R3. This acid deprotonates to form the bicarbonate ion ($HCO^{-}_{3(ac)}$) and subsequently the carbonate ion ($CO^{=}_{3(ac)}$), as it is depicted in reactions R4 and R5.

$$2H_2O_{(l)} \rightleftharpoons OH^{-}_{(ac)} + H_3O^{+}_{(ac)} \qquad \text{R1}$$

$$CO_{2(g)} \rightleftharpoons CO_{2(ac)} \qquad \text{R2}$$

$$CO_{2(g)} + H_2O_{(l)} \rightleftharpoons H_2CO_{3(ac)} \quad \text{R3}$$

$$H_2CO_{3(ac)} + H_2O_{(l)} \rightleftharpoons HCO^-_{3(ac)} + H_3O^+_{(ac)} \quad \text{R4}$$

$$HCO^-_{3(ac)} + H_2O_{(l)} \rightleftharpoons CO^=_{3(ac)} + H_3O^+_{(ac)} \quad \text{R5}$$

The chemical solubility of carbon dioxide refers to the amount of carbon dioxide that reacts and is in equilibrium with dissolved (physically absorbed) carbon dioxide. In the case of water as a chemical solvent, the chemical solubility is negligible compared to the physical solubility, which is greater than 99.5% at 25℃. This picture changes with the addition of an amine, where other reactions take place, such as carbamate formation and protonation of the amine, leading to higher chemical solubility than physical solubility. This point is discussed further in the next section.

In solubility experiments, there is no simple and accurate way to distinguish between the physical and chemical solubility of CO2. Since physical solubility is necessary to formulate and solve models based on mass transfer rate and kinetics, an alternative commonly taken is to measure the solubility of nitrous oxide (N2O) and establish parallelisms, this is called the N2O/CO2 analogy. N2O is a gas at standard conditions similar in structure, electronic arrangement, and molecular mass to carbon dioxide (LADDHA; DIAZ; DANCKWERTS, 1981), but with completely different chemical properties (SEVERIN, 2015) making it practically inert to the solvents and conditions used in carbon dioxide absorption. In this way, the Henry constant of nitrous oxide in the solvent is measured and converted to the Henry constant of carbon dioxide by multiplying by the ratio of the Henry constant for both gasses in water (Equation (3)).

$$H^{Solution}_{CO2} = H^{Solution}_{N2O} \cdot \frac{H^{Water}_{CO2}}{H^{Water}_{N2O}} \quad (3)$$

After making a judicious review of different studies on the solubility relationship of these two gases and their dependence on temperature, Monteiro 2015 et al. (MONTEIRO; SVENDSEN, 2015) concluded that there is no sound evidence for this relationship to be accurate for the concentrations used for industrial purposes, for example a 5 molar solution of MEA. However, it is a well-established approach in almost every assessment of aqueous amine solvents. Fortunately, we can use alternative models and computational approaches that can be used to estimate CO2 solubility, which are reviewed and discussed in the following sections.

2.2 TERTIARY AMINES AND TERTIARY ALKANOLAMINES AS CARBON CAPTURE SOLVENTS

Amines are organic compounds derived from ammonia, where one, two, or all three hydrogen atoms are replaced by carbon chains, called primary, secondary, or tertiary amines, respectively (WADE JR.; SIMEK, n.d.). In the case of alkanolamines, the carbon chain contains an alcohol group.

Amines possess a lone electron pair on the nitrogen atom and can function as nucleophiles. For instance, in an aqueous solution, they act as Brønsted-Lowry bases, deprotonating water and thereby increasing the pH. In a broader context, primary and secondary amines act as Lewis bases, directly reacting with electrophilic carbon atoms in carbon dioxide. Specifically, the nitrogen in primary and secondary amines is capable of initiating a nucleophilic attack on CO2, forming a zwitterionic carbamic acid, as it is shown in left side of Figure 2. This zwitterion is further stabilized through deprotonation by a base, which could be another amine molecule. A comprehensive investigation into this process was conducted by Kortunov et al. (KORTUNOV et al., 2016).

Figure 2 – Reaction mechanisms in aqueous solution for primary and secondary amines (left side) and for tertiary amines (right side).

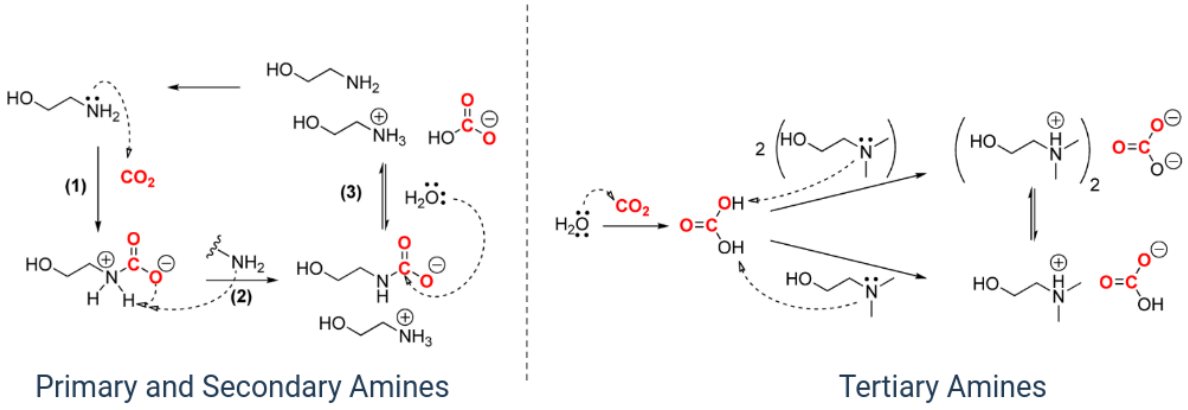

Source: Taken from (KORTUNOV et al., 2016).

On the other hand, in tertiary amines, the absence of hydrogen atoms makes the formation of zwitterion practically impossible, so in an aqueous solution they act as intermediates, the lone electron pair attacks the water molecules forming the protonated amine and hydroxyl ions (R6), thus promoting the subsequent formation of bicarbonate and carbonate (R4 and R5). Alternatevely they deprotonated the carbonic acid to form carbonate and bicarbonate as it is depicted in the right side of Figure 2.

$$R_1(R_2)NR_3 + H_2O \rightleftharpoons R_1(R_2)N^+HR_3 + OH^- \quad \text{R6}$$

$$R_1(R_2)NR_3 + R_4OH + CO_2 \rightleftharpoons R_1(R_2)N^+HR_3 + R_4OCOO^- \quad \text{R7}$$

$$2R_1(R_2)NCCOH \rightleftharpoons R_1(R_2)N^+HCCOH + R_1(R_2)NCCO^- \quad \text{R8}$$

In the absence of water, the above mentioned reaction is not possible. Therefore, it is commonly assumed that tertiary amines in pure or non-aqueous solutions act only as physical solvents (VERSTEEG; VAN SWAAIJ, 1988). However, recent studies using nuclear magnetic resonance (NMR) have shown that tertiary amines are capable of deprotonating the alcohol group and subsequently producing alkyl-carbonates, as it is depicted in reaction R7. For instance, Sen et al. (SEN et al., 2020) systematically studied blends of tertiary amines and ethylene glycol for carbon dioxide capture and hydrogenation to methanol.

The above mechanism is not possible in pure tertiary amines but is still possible in pure tertiary alkanolamines since they contain both the alcohol group and the amine group, so reaction R6 would be an autoprotonation reaction (R8). This phenomenon has not been studied in detail but was observed in pure DMEA (RAINBOLT et al., 2011), and briefly quantified in aqueous solutions of MEA, DEA, TEA, and MDEA (BEHRENS et al., 2017, 2019; CIESLAROVA; SANTOS; LAGO, 2018).

Regarding the advantages of using tertiary amines as solvents, one of the most attractive characteristics is their chemical stability. In this respect, Lepaumier et al. (LEPAUMIER; PICQ; CARRETTE, 2009; LEPAUMIER et al., 2010) performed thermal degradation studies in the presence and absence of dissolved carbon dioxide and concluded that both tertiary alkanolamines and tertiary diamines are more resistant to degradation than primary and secondary alkanolamines and diamines, the latter being the worst performers in this respect.

2.3 FORCE FIELDS AND MOLECULAR DYNAMICS

2.3.1 Force fields

The force fields are a mathematical expression for the internal energy of a system as a function of the positions of the particles that make up that system. Classical force fields usually sum several terms, each representing a molecular interaction. These interactions can be intramolecular or intermolecular, depending on whether they involve particles belonging to the same molecule or particles belonging to different molecules. The most common intramolecular terms include bond stretching, angle bending, and torsional rotations, which are interactions between pairs of atoms distanced by one, two, or three covalent bonds. A couple of atoms distanced by a chain of more than

three covalent bonds may still interact via intramolecular electrostatic and van der Waals interactions. The sum of these terms is known as the *intramolecular potential*. The *intermolecular potential* is then defined as the sum of the van der Waals and electrostatic interactions between pairs of atoms belonging to different molecules.

$$U_{total}(\{\mathbf{r}\}) = U_{intra}(\{\mathbf{r}\}) + U_{inter}(\{\mathbf{r}\}) \tag{4}$$

Force fields are typically composed of two main components: the mathematical equations that describe the potential energy of the system and a set of parameters that characterize the interactions between different atom types. These parameters are often derived from experimental data and quantum mechanical calculations and are essential for accurately representing the forces that govern molecular behavior. Widely used force fields include GAFF, CHARMM, GROMOS, OPLS, and TraPPE, each with its own specific set of equations and parameterization. Force fields can be classified according to the degree of detail in molecular modeling; thus, force fields that represent each atom of the system as a single particle are called all-atom (AA) force fields; if the atoms are grouped, it is called united-atom (UA) model (GONZÁLEZ, 2011). To exemplify this, Figure 3 shows a representation of the difference in the number of atomic sites for the monoethanolamine molecule where there is an economy of 4 atomic sites from model AA to model UA.

Figure 3 – 2D representation of a MEA moelcule in an UA model (left) and in a AA model (right).

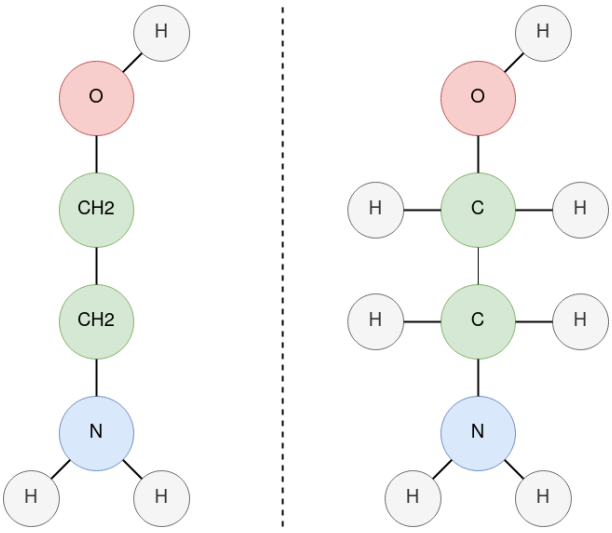

Source: The author.

2.3.2 Lennard-Jones potential

The Lennard-Jones potential is an effective approximation for representing van der Waals interactions. It is composed of two terms, the first positive term tries to recreate the highly repulsive short-range interactions arising from the overlap of the electronic cloud and the Pauli exclusion principle. In its most common form, it is a term raised to the twelfth power. The second term is the attractive potential term attempting to represent the medium-range interactions associated with the momentarily induced dipole arising from the dispersion of the electron cloud (ALLEN; TIDESLEY, n.d.; GONZÁLEZ, 2011). The Lennard-Jones potential is expressed by the Equation (5) and depicted dimensionless in the figure below.

Figure 4 – Dimensionless Lennard-Jones potential.

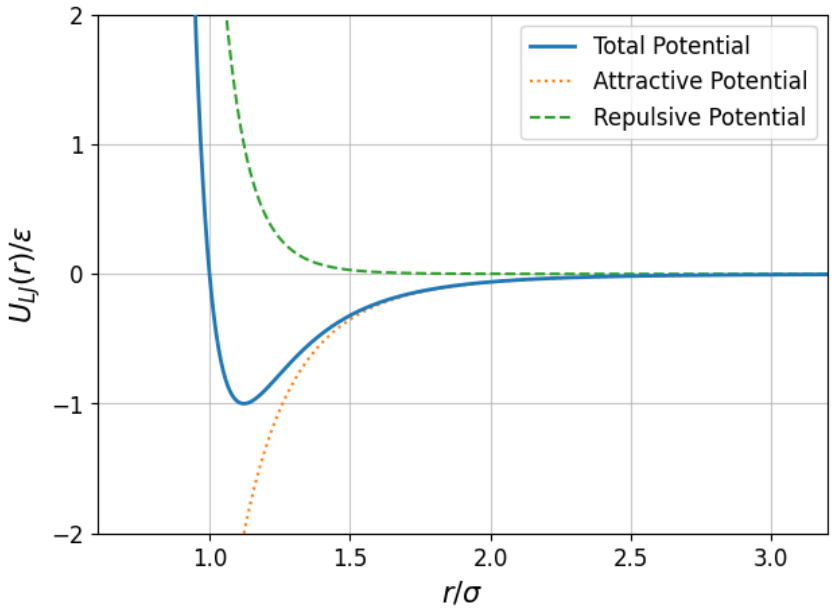

Source: The author

$$U_{\mathrm{LJ}}(r_{ij}) = 4\varepsilon_{ij}\left[\left(\frac{\sigma_{ij}}{r_{ij}}\right)^{12} - \left(\frac{\sigma_{ij}}{r_{ij}}\right)^{6}\right] \tag{5}$$

The parameters σ and ε represent the depth of the potential well and the distance at which the potential becomes zero. Each atomic site has a σ and ε parameter in the force field parameterization. The potential between a pair of unlike atoms is calculated using a weighting strategy between the parameters of each atomic site. This approach is called the combination rule. The arithmetic averages over σ, and the geometric averages over ε are a particular type of combination rules called Lorentz-Berthelot (Equation (6)).

$$\sigma_{ij} = \frac{\sigma_i + \sigma_j}{2} \tag{6a}$$

$$\varepsilon_{ij} = \sqrt{\varepsilon_i \varepsilon_j} \tag{6b}$$

Combination rules reduce the degrees of freedom in the parametrization of a force field. However the cross-interaction potential (intermolecular potential between unlike atom sites) may differ from that predicted by these combination rules and is, therefore, the most appropriate parameter to be tuned when studying mixtures.

2.3.3 Molecular dynamic simulations

Molecular simulations involve the motion of particles (thermal energy) to explore the potential energy surfaces approximated by the force field expression to study molecular systems dynamically, evolving in time as in the case of molecular dynamics simulations or sampling the possible motions of the system as in the case of Monte Carlo simulations. In molecular dynamic simulations, the Newtonian equations of motion are solved numerically for each particle of the system. The result of this procedure is the system's state variables over time, namely, the position, velocity, and force on each particle of the system and the system's internal energy at each time step. Analysis of these state variables employing statistical mechanics and molecular kinetic theory leads to calculating a wide variety of physicochemical properties (ALAVI, n.d.).

2.4 COMPUTATIONAL STUDIES ON CO2 PHYSICAL SOLUBILITY

According to Skyner et al., (SKYNER et al., 2015), three main categories exist for the computational calculation of solubilities: Informatic-based methodologies, implicit solvent free energy calculations, and explicit solvent free energy calculations. On the first front, QSPR, statistical, and machine learning methodologies (YANG, Z. et al., 2023) are used to predict solubility in physical solvents at ambient conditions (ORLOV et al., 2021), or as a function of temperature and pressure (LEMAOUI et al., 2023). There is also a wide range of work on this property in ionic liquids (SONG et al., 2020; ZHANG et al., 2023). Another way to calculate the free energy and, ultimately, the solubility is to embed the molecule in a homogeneous dielectric continuous medium that represents solvent (YANG, X. et al., 2017); this is the basis of free energy calculations in implicit solvents. Two models stand out in this respect, the SMD (LI et al., 2021; MALHOTRA et al., 2019) and COSMO (GONZALEZ-MIQUEL et al., 2012). The works are mainly focused predicting the relative free energies since, as Noroozi et al. (NOROOZI; SMITH, W. R., 2020a) point out, this kind of model still needs the accuracy to predict the solvation free energies adequately (CANTU et al., 2016). Therefore, these models have been preferred in the study of amine protonation constants (NOROOZI; SMITH, W. R.,

2020b), formation of reaction intermediates with carbon dioxide capture (MATSUZAKI et al., 2019), and stability of carbamate species (GANGARAPU; MARCELIS; ZUILHOF, 2013). However, studies have also been carried out for the calculation of Henry constants of carbon dioxide in aqueous solutions of ionic liquids and their mixtures with alkanolamines (BALCHANDANI, S.; SINGH, 2021; BALCHANDANI, S. C.; MANDAL; DHARASKAR, 2021).

Explicit solvent methods can represent the specific solute-solvent interactions. However, they tend to be computationally more expensive due to the high number of degrees of freedom (SKYNER et al., 2015). Many of these studies are centered on the solubility of carbon dioxide in ionic liquid solvents (BUDHATHOKI; SHAH; MAGINN, 2015; KAPOOR; SHAH, 2018), and some of them in deep eutectic solvents (AL-FAZARI et al., 2023). Regarding tertiary amine solubilities, Rozanska et al. (ROZANSKA; WIMMER; MEYER, 2021) calculated the solubility of carbonate ion and protonated amine in aqueous solution by means of molecular dynamic simulations and then calculated the equilibrium constant of the reaction and estimated the reaction rate. Orlov et al. (ORLOV et al., 2022) used the same approach to systematically select tertiary amine-based solutions for carbon dioxide capture. Although the method of calculation of the free energy was not specified, the authors claimed high accuracy in each of their schemes. The free energy calculation method BAR was utilized by Norozi et al. (NOROOZI; SMITH, W. R., 2020a) to compute henry coefficients and solve the chemical and phase equilibria of non-experimentally studied amine systems. This method has also been used more specifically to study the behavior of the henry constant as a function of temperature for solvents based on polyamines (JUNG et al., 2020). In explicit solvent methods, the number of particles must be sufficient to ensure that the solvated molecule does not interact with itself and that the solvent settling layers around the molecule are properly recreated. Although the encountered studies resulted in box sizes exceeding 2 times the cutoff radius, no studies on fixed size effects have been reported to date.

Continuous Fractional Component Monte Carlo techniques were also used to compute the solubility of flue gasses, including CO2, in commercial physical solvents (CHEN; RAMDIN; VLUGT, 2023), several all atoms force field were used in systems as big as 250 molecules, deviations range from 2% until 60% in the reproduction of henry coefficient of carbon dioxide. Using this MC technique, Danwass el al. (DAWASS et al., 2021) found that adjustment may be done in order to increase the moderate underpredictions obtained on henry constant of flue gasses in MEG modeled by Trappe-UA force field. In regard to amines, Chen et al. (CHEN et al., 2014) computed the henry constant on aqueous solution of MEA with all atom OPLS force field, although the CO2 solubility experimental data on primary amines is not experimentally accessible, they found deviations between 20% and 50% in the henry constant of N2O.

Orozco et al. (OROZCO; LACHET; MACKIE, 2016) used the Widom test par-

ticle insertion method over MonteCarlo simulation to determine the excess chemical potential of some greenhouse gasses in pure and aqueous solutions of amines and alkanolamines using the AUA4 force field. They took advantage of the nitrous oxide solubility data to adjust the intermolecular cross-interaction parameters so that they obtained a potential capable of recreating the solubility of this gas in aqueous amine solutions. In a similar trend Konhs et al. (KOHNS et al., 2017) scaled the intermolecular cross-interaction parameters of an specific ethanol anisotropic united atom force field (SCHNABEL; VRABEC; HASSE, 2005) to recreate the henry constants of CO2 and N2O in aqueous ethanol solution to computationally test the CO2/N2O analogy. In both of the above works deviations less than 8% were obtained after the adjustment process.

In view of the previously mentioned works, the united atom AUA4 force field was selected to model the organic substances because: (i) The work of Orozco et al. shows a good precedent in the reproduction of the thermodynamic and transport properties of this force field in relation to amines (OROZCO et al., 2014) and alkanolamines (OROZCO et al., 2013), as well as the study of the intermolecular interactions in aqueous systems of these substances. (ii) Because it is a transferable, anisotropic and united atom force field it promises to reduce computational times without losing physical detail. This model was parameterized to study a relatively large set of functional groups: linear(UNGERER et al., 2000) and branched alkanes(BOURASSEAU et al., 2002), cycloalkanes(BOURASSEAU; UNGERER; BOUTIN, 2002), aromatic and polyaromatic compounds(CONTRERAS-CAMACHO et al., 2004b, 2004a; AHUNBAY et al., 2005), olefins(BOURASSEAU et al., 2003), alcohol and polyalcohols(FERRANDO et al., 2009), ethers(FERRANDO et al., 2011), aldehydes, ketones(FERRANDO; LACHET; BOUTIN, 2010), esters(FERRANDO; LACHET; BOUTIN, 2012), carboxylic acids(FERRANDO et al., 2013), amines(OROZCO et al., 2011, 2012, 2014) and alkanolamines(OROZCO et al., 2013). Aquing et al. (AQUING et al., 2012) and Yiannourakou et al. (YIANNOURAKOU et al., 2013) have shown the predictive power of AUA4 by assessing several thermodynamic, structural, and dynamics properties. Therefore the methodology section will describe this force field and its particularities.

2.5 AVAILABLE EXPERIMENTAL DATA

An exhaustive search of the scientific literature was carried out using the SCOPUS and Google Scholar search engines using different combinations of the terms: ‘tertiary amine’, ‘henry constant’, ‘co2’, ‘physical solubility’ and ‘carbon dioxide’. A large amount of information was found for total solubilities (physical solubility in conjunction with physical solubility) however the physical solubility data isolated is much reduced. In addition, an abundance of nitrous oxide physical solubility data was found, which by analogy are then converted to carbon dioxide solubility by the N2O/CO2 analogy. These data were used only for comparison and discussion.

Abu-Arabi et al. (ABU-ARABI et al., 2001) measured the adsorbed carbon dioxide in acidic solutions of triethanolamine up to compositions of 30% in mass, because of the excess of hydronium ions the chemical equilibrium, described by equation R6, is shifted to the reagents and theoretically the absorbed carbon dioxide is merely by physical interactions. On the other hand Kierzkowska-Pawlak et al. (KIERZKOWSKA-PAWLAK; ZARZYCKI, 2002) mixed the tertiary amine MDEA with ethanol and measured the solubility of carbon dioxide in this mixture. This amine was later studied by Skylogianni et al. (SKYLOGIANNI et al., 2020) and Orlov et al. (ORLOV et al., 2021) who measured the solubility of MDEA as a pure component, and also as function of the partial carbon dioxide pressure. Additionally they measured the solubility in NMM and EDEA at ambient temperature and as a function of the partial CO2 pressure, they also report a value for the tertiary amine TRE. Rainbolt et al. (RAINBOLT et al., 2011) estimated the amount of carbon dioxide absorbed physically and chemically on DMEA, DIPEA and DEA by NMR spectrograms. Finally, data of CO2 solubility in pure TEA as a function of pressure at 4 different temperatures were recently published (JOU; MATHER, 2023). Table 1 summarizes these findings.

Table 1 – Experimental information available for physical solubility of CO2 in tertiary amines.

System	HLC range	Temperature range	Data points	Technique	Reference
TEA aqueous solutions	140 MPa - 300 MPa	293.15 K - 333.15 K	18	Protonation method	(ABU-ARABI et al., 2001)
MDEA and EtOH solutions	0.7 MPa - 16.3 MPa	293.15 K	9	Equilibirum cell	(KIERZKOWSKA-PAWLAK; ZARZYCKI, 2002)
Pure MDEA	1.4 MPa - 34 MPa	303.15 K - 393.15 K	10	Equilibrium cell	(SKYLOGIANNI et al., 2020)
Pure MDEA	1.0 MPa	298.15 K	1	Equilibrium cell	(ORLOV et al., 2021)
Pure EDEA	1.3 MPa	298.15 K	1	Equilibrium cell	(ORLOV et al., 2021)
Pure NMM	3.8 MPa	298.15 K	1	Equilibrium cell	(ORLOV et al., 2021)
Pure TRE	4.4 MPa	298.15 K	1	-	(ORLOV et al., 2021)
Pure DMEA	8.6 MPa	298.15 K	1	Estimated from NMR	(RAINBOLT et al., 2011)
Pure DIPEA	14.8 MPa	298.15 K	1	Estimated from NMR	(RAINBOLT et al., 2011)
Pure DEEA	9.8 MPa	298.15 K	1	Estimated from NMR	(RAINBOLT et al., 2011)
Pure TEA	0.8 MPa - 48.9 MPa	323.15 K - 398.15 K	4	Equilibrium cell	(JOU; MATHER, 2023)

Source: The author.

3 METHODOLOGY

3.1 AUA4 FORCE FIELD

In general terms, the AUA4 force field represents a collapse of the hydrogen atoms of the carbon chain into a single atomic site (united atom condition), whose center of force for the Lennard Jones interactions is displaced away from the center of mass of the united atom (anisotropy condition). This displacement is such that it compensates for the absence of the carbon chain hydrogens and ends up better recreating the behavior of the electron cloud, So the parametrization of the force field contains a third parameter called delta, the distance between center of atom and center of force for dispersive-repulsive interactions. Another peculiarity of this force field is that its parameterization procedure was performed on the vapor pressure, in addition to the density and the vaporization enthalpy, leading to a more robust recreation of physicochemical properties. For further clarity, Figure 5 shows the representation of a methyldiethanolamine (MDEA) molecule.

Figure 5 – Molecular structure (left) and AUA4 molecular representation (right) of methyldiethanol amine molecule. Green spheres represent the shifted force center, typical of the AUA model.

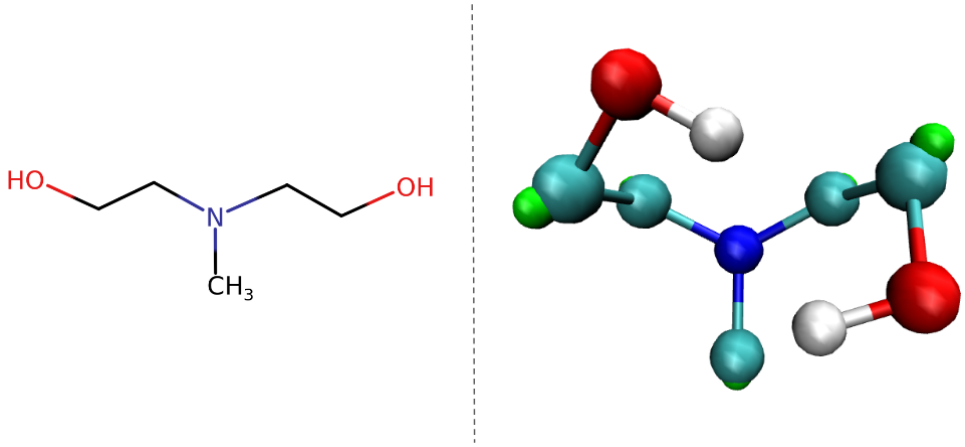

Source: The author.

In the AUA4 force field the intermolecular potential (Equation (7)) has two terms: that of the electrostatic interactions represented by the Coulomb law and that of the repulsive dispersion forces modeled by the Lennard-Jones potential.

$$U_{inter} = \frac{q_i q_j}{4\pi\varepsilon_0 r_{ij}} + 4\varepsilon_{ij}\left[\left(\frac{\sigma_{ij}}{r_{ij}}\right)^{12} - \left(\frac{\sigma_{ij}}{r_{ij}}\right)^{6}\right] \tag{7}$$

The crossed Lennard Jones parameters are obtained according to the Lorentz-Berthelot combining rules (Equation (6)).

On the other hand, the intramolecular potential (Equation (8)) contains the bending and torsion dihedral terms. Meanwhile, the distance of the bonds is kept fixed. The intramolecular van der waals and electrostatic interactions are only considered for atoms distanced by more than 3 bonds.

$$U_{intra} = \frac{1}{2}k_{bend}(\cos\theta - \cos\theta_0) + \sum_{n=0}^{8} a_n[\cos(\varphi + \pi)]^n \tag{8}$$

where k_{bend}, θ_0 and φ are the bending constant, the angle of equilibrium and dihedral angle respectively.

3.2 CARBON DIOXIDE FORCE FIELD

The carbon dioxide molecule was modeled and simulated with the ZHU model (ZHU et al., 2009).This model was selected based on the study of Cao et al. (CAO et al., 2022), who shows that within the common carbon dioxide force fields ZHU model is the best to reproduce the phase equilibria and transport properties. Additionally ZHU model overperformed the well known TraPPE model in the phase behavior near the critical conditions of the carbon dioxide.

ZHU models explicitly represent oxygen and carbon atoms, the bond distances are kept constant while the bond angle varies according to a harmonic potential (Equation (9)), which gives it a flexible character. The parameters of this model are presented in the table 2 The electrostatic interactions are calculated by Coulomb's law and the repulsion dispersion interactions follow the Lennard-Jones potential (Equation (7)), for the cross interactions the Lorentz Berthelot combining rules are used (Equation (6)).

$$U_{Intramolecular} = \frac{1}{2}k_{bend}(\theta - \theta_0) \tag{9}$$

Table 2 – Parameters of ZHU potential of carbon dioxide.

Parameter	Units	Value
ε_C	kJ/mol	0.23397
ε_O	kJ/mol	0.66824
σ_C	nm	0.28
σ_O	nm	0.3028
q_C	ev	0.6516
q_O	ev	-0.3258
θ_{O-C-O}	deg	180
k_{bend}	kJ/(mol-nm2)	110

Source: Retrieve form (ZHU et al., 2009).

3.3 GENERAL SIMULATION DETAILS

The open source molecular dynamics software GROMACS (ABRAHAM et al., 2015) version 2022.3 was used. The newton equations were integrated by the leap-frog algorithm using a time step of 0.002 ps. The calculation of van Der Waals and electrostatic interactions were truncated at a distance of 1.2 nm. To correct for the long-range effects of this option, the pressure and energy correction was used for the attractive forces of the van Der Waals potential. For the long-range electrostatic interactions we used the particle mesh Ewald algorithm with an interpolation of order 4. Velocity rescaling with a stochastic term (v-rescale GROMACS option) was used as a thermostat in canonical ensemble (NVT) and isobaric-isothermal ensemble (NPT). In the latter, exponential relaxation pressure coupling with a stochastic term (C-rescale GROMACS option) was used as a barostat.

3.3.1 Evaluation of AUA4 force field

The inclusion of the anisotropic characteristics of the AUA4 force field in the GROMACS software was performed by means of virtual sites. Thus, for each bonded carbon atom or for each heteroatom a virtual site was assigned with no mass, no charge but with van der waals interactions, located in the direction and at the delta distance stipulated by the force field parameterization. The creation of the topology and coordinate files was automated using a python routine that was made available in an open github repository and named AUA4GRO. This methodology and results of this subsection was recently published in Journal of Physical Chemistry A and are partly reproduced here with permission from J. Phys. Chem. A 2023, 127, 1555-1563 Copyright 2023 American Chemical Society (DOI: doi.org/10.1021/acs.jpca.2c08335).

The evaluation of the implementation was performed on the vapor-liquid equilibrium properties of a representative group of 19 substances containing the functional groups alkane, alcohol, ether, ester, carboxilic acid, ketone, aldehyde, amine and alkanolamine. The identifier of each substance along with the evaluated saturation temperature is presented in Table 3. The evaluation was performed using the following three steps simulation scheme (Figure 6): (i) The explicit vapor-liquid interface simulation was carried out in slab geometry, obtained from enlarging an equilibrated box containing 1053 molecules along the z-direction. Such molecules were located by replicating the coordinate file, obtained from AUA4GRO, through the GROMACS command “genconf”. Further, the slab-like box was equilibrated at the desired temperature and constant volume (NVT ensemble) for 4 ns. The analysis was performed over a production stage of 4 ns in the same equilibration conditions. (ii) The vapor phase was simulated in an NVT ensemble by randomly placing at least 30 molecules or as many molecules which do not exceed a cubic box edge of 7 nm. The box size was computed from the vapor

Table 3 – Name, SMILES code, CAS number, normal boiling point [K], critical temperature [K], and temperatures corresponding to the three thermodynamic conditions simulated.

Molecule name	**SMILES code**	**CAS**	**Normal boiling point**	**Critical temperature**	**T1**	**T2**	**T3**
methyl alcohol	CO	67-56-1	337.8	513	375	425	450
ethyl alcohol	CCO	64-17-5	351.5	514	325	375	425
1-hexanol	CCCCCCO	111-27-3	430	610.5	450	500	550
ethylene glycol	OCCO	107-21-1	470.5	720	500	550	600
dimethyl ether	COC	115-10-6	249.5	401	260	300	340
acetone	CC(=O)C	67-64-1	329.3	508	340	380	420
2-pentanone	CCCC(=O)C	107-87-9	375	561.1	380	420	460
acetaldehyde	CC=O	75-07-0	294	466	320	360	400
pentanal	CCCCC=O	110-62-3	376	568.3	380	420	460
acetic acid	CC(=O)O	64-19-7	391.2	593	425	475	525
methyl amine	CN	74-89-5	266.8	430.85	300	350	400
dimethyl amine	CNC	124-40-3	281	437.22	290	330	370
trimethyl amine	CN(C)C	75-50-3	275	433.2	280	320	360
1–hexylamine	CCCCCCN	111-26-2	403	589.14	465	500	540
di-n-propylamine	CCCNCCC	142-84-7	383	555.8	375	430	470
monoethanolamine	OCCN	141-43-5	443.2	671.4	450	500	550
ethylenediamine	NCCN	107-15-3	391.2	613.1	425	500	550
pentane	CCCCC	109-66-0	309.2	469.8	300	360	420
decane	CCCCCCCCCC	124-18-5	447.2	617.8	400	450	500

Source: The author.

density obtained from the two-phase simulation. The simulation production time was 2 ns, preceded by a 1 ns equilibration simulation. (iii) The liquid-phase simulation was performed by placing 343 molecules in an isobaric-isothermal ensemble. The pressure was set equal to the zz component of the pressure tensor in the two-phase simulation (i.e., vapor pressure).

As a particularity, on simulation of two-phase Lennard Jones Particle mesh ewald (LJPME) algorithm was applied for the computation of long range dispersion-repulsive interactions due to the inhomogeneity on the radial distribution of the molecules near to the interface.

To obtain the liquid and vapor densities we first divided the tow-phase simulation box of production stage into 240 equally spaced portions along the z-axis, giving rise to 0.1 nm thick slices (24 nm divided into 240 pieces), for which the density was calculated, resulting in a density profile along the z-axis. Such profile was subsequently adjusted to an hyperbolic tangent expression given by Equation (10). Where the density of each phase appears as a fitting parameter along with the thickness of the interface and a characteristic distance.

$$\rho(z) = \frac{1}{2}(\rho^{l} + \rho^{v}) - \frac{1}{2}(\rho^{l} - \rho^{v}) \tanh \frac{2(z - z_0)}{d} \tag{10}$$

As was mentioned above, vapor pressure was obtained from the mean value of the pressure component in the z-direction as retrieved in similar studies(ARRIOLA

GONZÁLEZ et al., 2022; MORROW; HARRISON, 2019; TOUTOUNI; KUBELKA; PIRI, 2022). The vaporization enthalpy was calculated from the differences in internal energy from the simulation of the vapor phase and liquid phase and the corresponding PV term.

$$\Delta h^{vap} = h^{v} - h^{l} = U^{v} - U^{l} + P_{sat}(V_m^V - V_m^l) \tag{11}$$

3.3.2 Optimization of intermolecular potential (AUA4 - ZHU)

For the optimization and validation scheme (Figure 7), two types of simulations were performed, all corresponding to single-phase systems, either the solvent in sub-cooled liquid conditions or the solvent and carbon dioxide in supercritical conditions. The two simulation procedures are described below.

Simulation for excess enthalpy and excess molar volume: The initial box was obtained by randomly placing 1000 molecules of carbon dioxide and solvent satisfying the molar concentration for each case. The size of the box was such that the mass density was 400 kg/m3. This box was then equilibrated in a NPT ensemble at the temperature and pressure of each test for 2 ns and then passed to the NPT production stage for 1 ns. Equations for the calculation of this two properties are shown below:

$$V_m = \frac{V}{N/N_A} \tag{12}$$

$$h = U + P * V_m \tag{13}$$

$$V_m^{excess} = V_m - x_i \cdot V_{i,m} - x_j \cdot V_{j,m} \tag{14}$$

$$h^{excess} = h - x_i \cdot h_i - x_j \cdot h_j \tag{15}$$

Simulation for Henry law constant calculation: The initial simulation box was created by putting a CO2 molecule in the center of an empty box and then randomly placing 1000 molecules of the solvent. The size of the initial box was chosen so that the initial mass density was 600 kg/m3 which ensures that molecules, even if randomly placed, do not have high energy interactions or ‘miscontacts’ among them. From the initial box, 4 independent 0.5 ns NVT equilibrations were run using 4 random velocity generation seeds. Each box was equilibrated at working temperature and atmospheric pressure for 1 ns in an NPT ensemble. By monitoring the total energy and density it was verified that equilibrium was reached within the first 0.1 ns. The equilibrated box is then used with each of the 20 different CO2 lambda coupling factors and goes through an energy minimization, NVT equilibration, NPT equilibration and finally NPT

production, from which the statistics for the energy calculation are obtained. Equations for the calculation of this property from ensemble variables are shown below:

$$\mu^{excess} = \mu^{excess}_{vDw} + \mu^{excess}_{coul.} \tag{16}$$

$$\mu^{excess}_{vDw/coul.} = \sum \Delta G_{\lambda_i \rightarrow \lambda_j} \tag{17}$$

$$H = \rho \cdot R \cdot T \cdot exp\left(\frac{\mu^{excess}}{R \cdot T}\right) \tag{18}$$

Table 4 – Supercritical data utilized to optimization procedure.

Interaction site	Description	Molecule	T [K]	P [bar]	Reference
-CH3	Primary carbon	Ethane	272 - 308	110	(WORMALD; EYEARS, 1988)
-CH2-	Secondary carbon	Hexane	308 - 313	105	(TOLLEY; IZATT; OSCARSON, 1991)
-O(H)	Hydroxy oxygen	Ethanol	308 - 323	75 - 105	(CORDRAY et al., 1988; CUNICO; TURNER, 2017)

Source: The author.

The parameters to be optimized were the cross-interaction parameters of the Lennard Jones potential between the atomic sites of the organic compounds and the carbon dioxide oxygen site. The optimization was performed on 3 atomic sites, for a total of 6 parameters to be optimized. This optimization was performed sequentially, with a delicate selection of experimental data, such that a set of parameters was optimized for an atomic site in a representative molecule and transferred to a following molecule and a following optimization process. The experimental data were selected in such a way that the thermodynamic values of temperature and density are as close as possible to those that would be obtained under absorption conditions, i.e., temperatures close to the ambient temperature and densities at or above 700 kg/m3, if possible. The atomic groups to be optimized, the reprsentative molecule and the selected experimental conditions are shown in Table 4. The optimization consists in the minimization of the variance-weighted quadratic difference between experimental and predicted properties (Equation (19)). Ultimately this results in solving a system of equations as follows:

$$F_{OBJ} = \frac{1}{n}\sum_{i=1}^{n}\frac{(f_{Sim,i} - f_{Exp,i})^2}{s^2_{Sim,i} + s^2_{Exp,i}} \tag{19}$$

Deriving,

$$\frac{\partial F_{OBJ}}{\partial y_j} = \frac{1}{n}\sum_{i=1}^{n}\frac{2(f_{Sim,i} - f_{Exp,i})\frac{\partial f_{Sim,i}}{\partial y_j}}{s^2_{Sim,i} + s^2_{Exp,i}} \tag{20}$$

Applying the Taylor expansion, we get:

$$\frac{\partial F_{OBJ}}{\partial y_j} = \frac{1}{n}\sum_{i=1}^{n} \frac{2(f_{Sim,i0} - f_{Exp,i} + \sum_{k=1}^{p} \frac{\partial f_{Sim,i}}{\partial y_k}\Delta y_k)\frac{\partial f_{Sim,i}}{\partial y_j}}{s^2_{Sim,i} + s^2_{Exp,i}} \tag{21}$$

$$0 = \frac{1}{n}\sum_{i=1}^{n} \frac{2(f_{Sim,i0} - f_{Exp,i} + \frac{\partial f_{Sim,i}}{\partial y_1}\Delta y_1 + \frac{\partial f_{Sim,i}}{\partial y_2}\Delta y_2)\frac{\partial f_{Sim,i}}{\partial y_j}}{s^2_{Sim,i} + s^2_{Exp,i}} \tag{22}$$

Disagreeing

$$0 = \frac{2}{n}\sum_{i=1}^{n}\left(\frac{(f_{Sim,i0} - f_{Exp,i})\frac{\partial f_{Sim,i}}{\partial y_j}}{s^2_{Sim,i} + s^2_{Exp,i}}\right) + \frac{2}{n}\sum_{i=1}^{n}\left(\frac{\frac{\partial f_{Sim,i}}{\partial y_1}\Delta y_1 \frac{\partial f_{Sim,i}}{\partial y_j}}{s^2_{Sim,i} + s^2_{Exp,i}}\right) + \frac{2}{n}\sum_{i=1}^{n}\left(\frac{\frac{\partial f_{Sim,i}}{\partial y_2}\Delta y_2 \frac{\partial f_{Sim,i}}{\partial y_j}}{s^2_{Sim,i} + s^2_{Exp,i}}\right) \tag{23}$$

$$0 = \frac{2}{n}\sum_{i=1}^{n}\left(\frac{2(f_{Sim,i0} - f_{Exp,i})\frac{\partial f_{Sim,i}}{\partial y_j}}{s^2_{Sim,i} + s^2_{Exp,i}}\right) + \frac{2}{n}\sum_{i=1}^{n}\left(\frac{\frac{\partial f_{Sim,i}}{\partial y_1}\frac{\partial f_{Sim,i}}{\partial y_j}}{s^2_{Sim,i} + s^2_{Exp,i}}\right)\cdot\Delta y_1 + \frac{2}{n}\sum_{i=1}^{n}\left(\frac{\frac{\partial f_{Sim,i}}{\partial y_2}\frac{\partial f_{Sim,i}}{\partial y_j}}{s^2_{Sim,i} + s^2_{Exp,i}}\right)\cdot\Delta y_2 \tag{24}$$

Which can be read more clearly as

$$0 = a_j + b_j \cdot \Delta y_1 + c_j \cdot \Delta y_2 \tag{25}$$

This optimization was performed on 4 experimental data of excess enthalpy and excess volume at two different temperature and pressure conditions, for a total of 16 experimental data. The partial derivatives of the predicted properties were calculated with the centered finite difference approximation as shown in equation (26). The initial values of the optimization parameters were the ones obtained through the Lorentz Berthelot combining rules. The optimization procedure was stopped once the variation of the optimization parameters simultaneously did not change more than 0.004.

$$\frac{\partial f}{\partial y} = \frac{f(y + \delta y) - f(y - \delta y)}{2\delta y} \tag{26}$$

Figure 6 – Simulation scheme. Circles stand for thermodynamic properties. Rectangles stand for simulation stages.

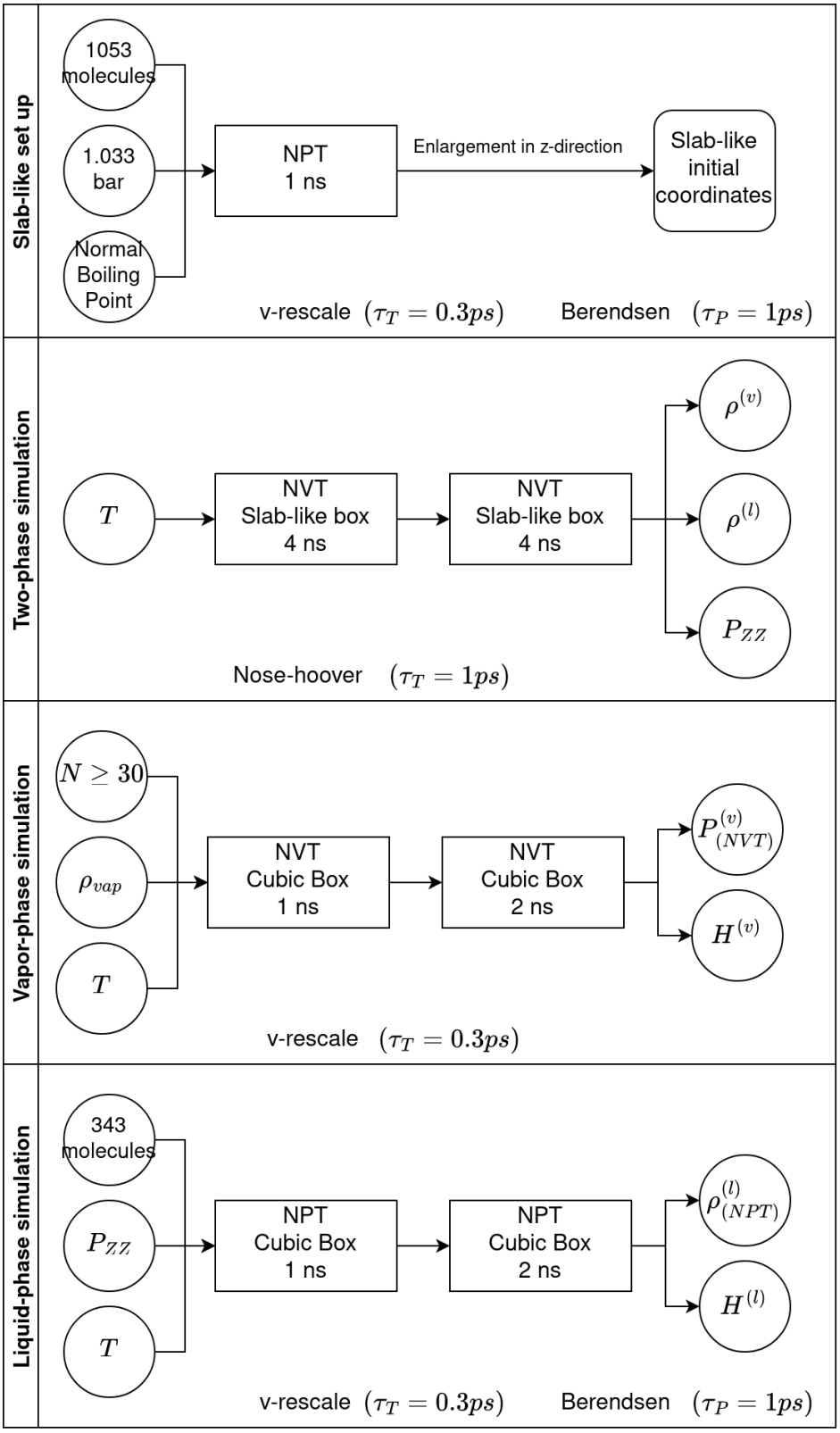

Source: Retrieve from (CASTRO ANAYA; GÓMEZ; OROZCO, 2023).

Figure 7 – Sequential optimization scheme by means of excess properties.

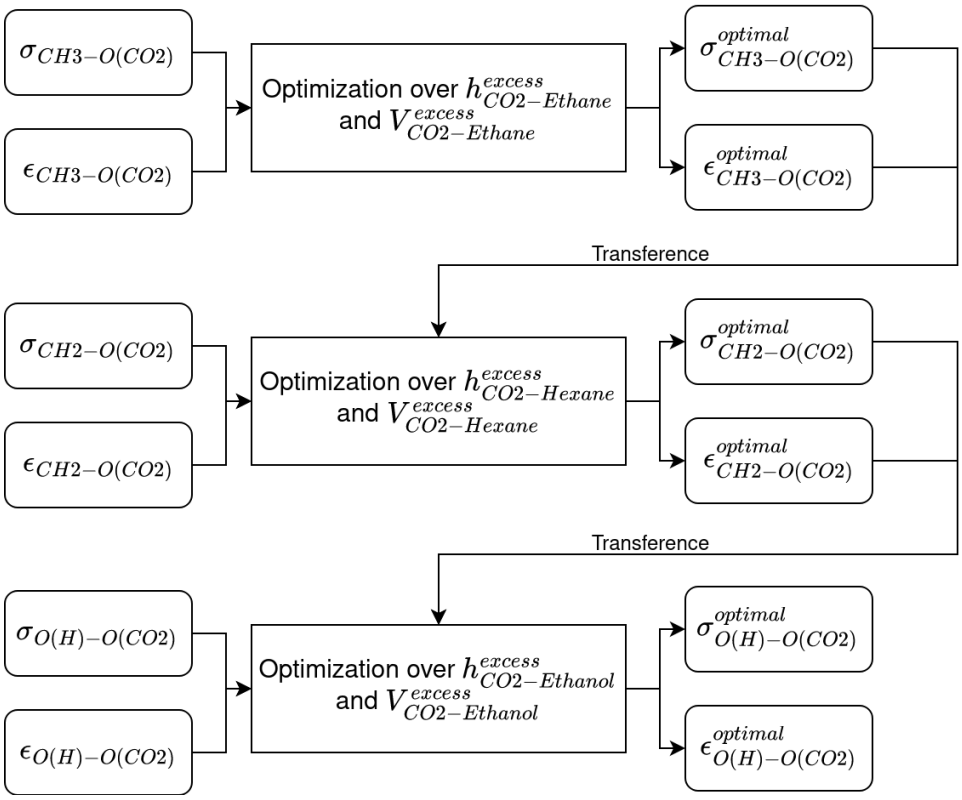

Source: The author.

4 RESULTS

4.1 ANALYSIS OF EXPERIMENTAL DATA

One of the main parts of this work is the optimization of the molecular model and validation with experimental data, therefore it is necessary to critically discuss these data in order to make appropriate decisions and pertinent conclusions. Disregarding the formation reaction of alkyl carbonates in pure tertiary amines can lead to a poor determination of the Henry's law constant, and the presence of water, even in small amounts, can lead to the formation of carbonate ions and also mask the true Henry's law constant. This first argument is evidenced by the Rainbolt et al. (RAINBOLT et al., 2011) data in which, if the formation of alkyl carbonate is disregarded, the carbon dioxide concentration can be misinterpreted and lead to Henry's law constant up to 4 times lower than the constant obtained considering this chemical reaction. Additionally, the trend indicates that as the pressure decreases, the magnitude of this phenomenon seems to increase, as can be seen in table 5.

Table 5 – Carbon dioxide solubility obtained from high pressure NMR measurements taken from (RAINBOLT et al., 2011).

P_{CO2} [MPa]	$x_{CO2}^{physical}$	x_{CO2}^{total}	$\frac{x_{CO2}^{total}}{x_{CO2}^{physical}}$
0.69	0.06	0.23	3.83
1.38	0.15	0.37	2.47
2.07	0.20	0.44	2.20
3.45	0.19	0.45	2.37

Source: The author.

Henry's law must satisfy Equation (1), which indicates that the absorption isotherms are linear functions with respect to the fugacity of the gas and must pass through the origin. To verify this linear behavior we regress the logarithm isotherm data and perform linear regression. In this sense a linear behavior should show a slope of 1 and the independent term corresponds to a logarithm of the Henry's law constant, as expressed in equation 4.1. Fugacity was calculated from the Peng-robinson equation of state and the poynting factor was computed utilizing the antoine equation for the vapor pressure of the solvent. The linear regression results are shown in Table 6.

$$ln\left(f_{CO2}\right) - \frac{\overline{v}_{CO2}^{\infty} \cdot \left(P - P_{solvent}^{(sat)}\right)}{RT} = ln\left(H_{CO2,solvent}\right) + ln(x_{CO2}) \tag{27a}$$

$$Y = ln\left(f_{CO2}\right) - \frac{\overline{v}_{CO2}^{\infty} \cdot \left(P - P_{solvent}^{(sat)}\right)}{RT} \tag{27b}$$

$$X = ln(x_{CO2}) \tag{27c}$$

$$b = ln\left(H_{CO2,solvent}\right) \quad (27)d$$

Table 6 – Carbon dioxide solubility obtained from high pressure NMR measurements.

Molecule	T [K]	m	b	R^2
TEA	323.15	1.4833	3.0791	0.9989
TEA	348.15	1.2379	3.3823	0.9999
TEA	373.15	1.1220	3.6183	0.9985
TEA	398.15	1.0902	3.8999	0.9996
MDEA	298.15	1.1197	0.3265	0.9974
MDEA	313.15	1.0947	1.3711	0.9996
MDEA	343.15	1.0204	2.3639	0.9920
EDEA	298.15	1.1476	0.7416	0.9885
NMM	298.15	1.0044	1.3469	0.9996

Source: The author.

Figure 8 – Logarithm of dissolved carbon dioxide mole fraction against the logarithm of the pressure-corrected fugacity for the TEA and the NMM.

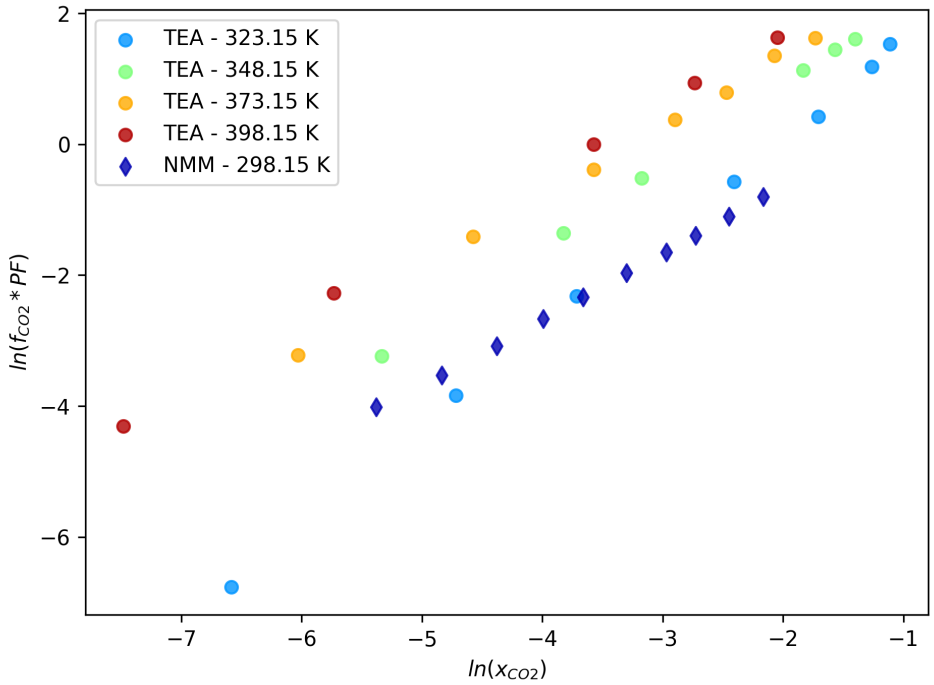

Source: The author.

The slope evidences a nonlinear behavior on alkanolamine substances that increases as temperature is lower, this could be related with the formation of carbonates and alkyl carbonates as both are exothermic equilibrium reactions, and therefore reactions favored at lower temperatures. This is particularly notorious in triethanolamine data and in some cases the slope reaches a linear behavior as shows the MDEA

isotherm at 343.15 K. On the other hand, The tertiary amine NMM shows a pretty linear behavior at low temperature. These data results should be treated with caution as they are a simple adjustment of a simplified model subject to statistical errors, however, they reflect an atypical behavior of alkanolamines systems at low temperatures. For comparison, Figure 8 shows a logarithmic plot of the molecules with the highest and lowest atypical behavior.

Based on this analysis, we selected the molecules NMM and TRE to assess the Henry's law coefficient computation. These two molecules are tertiary amines that theoretically have no mechanism available to react with CO2 and experimentally show no signs of reaction. We also will utilize MDEA data at 343 kelvin and higher temperatures supposing it show no signs of reaction either, which is possible because the reaction of alkyl carbonate formation is exothermic and therefore disadvantaged by temperature, so the apparent Henry's law constant should be close to the actual one.

4.2 EVALUATION OF THE AUA4 IMPLEMENTATION

The accuracy of the implemented force field for the calculation of equilibrium properties (liquid density, vaporization enthalpy and vapor pressure) was evaluated as the average absolute deviation (Equation (28)) and it is shown graphically in the figure 9.

$$\%\text{AAD} = \frac{abs(f_{Pred.} - f_{Exp.})}{f_{Exp.}} \tag{28}$$

In general, there was a high level of agreement observed for various properties, with deviations of approximately 2.13% for density, 4.91% for enthalpy of vaporization, and 8.30% for vapor pressure. To compare the performance of this force field implementation with results from other force fields of similar physical detail, the RMSD (Equation (29)) of each of the properties was calculated and shown in the following table.

$$\text{RMSD} = \sqrt{\frac{1}{n}\sum_{i=1}^{n} \| f_{Pred.} - f_{Exp.} \|^2} \tag{29}$$

Table 7 – Comparison of accuracy of force fields for predicting equilibrium properties.

Force Field	RMSD RhoL [kg/m3]	RMSD PVap [bar]	RMSD HVap [kJ/mol]	Substances assessed	Number of conditions assessed	Reference
GAFF	88.5	-	12.4	156	1	(FISCHER et al., 2015)
OPLS	43.6	-	8.1	156	1	(FISCHER et al., 2015)
CGenFF	38.8	-	6.6	156	1	(FISCHER et al., 2015)
TraPPE-UA	14.3	-	2.5	41	1	(NÚÑEZ-ROJAS et al., 2018)
AUA4	17.0	0.96	1.3	18	3	(CASTRO ANAYA; GÓMEZ; OROZCO, 2023)

Source: Retrieved from (CASTRO ANAYA; GÓMEZ; OROZCO, 2023).

Figure 9 – Absolute average deviation (AAD) of MD results on saturated liquid density (blue), enthalpy of vaporization (orange), and vapor pressure (red) for each molecule. Dotted lines indicate the %AAD over the entire set of molecules.

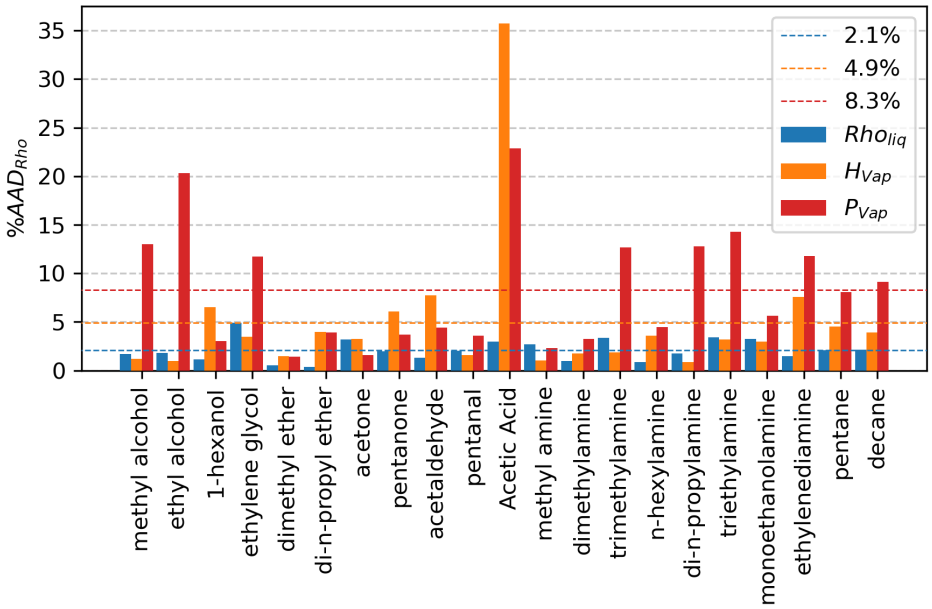

Source: Retrieved from (CASTRO ANAYA; GÓMEZ; OROZCO, 2023).

The AUA4 force field stands out for its very low error in the calculation of the vaporization enthalpy compared to the other molecular models, indicating that there is a good representation of the internal energy of the studied molecules, except for acetic acid. This discrepancy is not unique to the AUA4 force field and is in fact due to an overstabilization of the vapor enthalpy, associated with the inability to adequately recreate the short range forces and dimer formation in the vapor phase in short chain carboxylic acids, a detailed analysis can be found in the supplementary information of (CASTRO ANAYA; GÓMEZ; OROZCO, 2023). In relation to density the AUA4 force field performs well just behind the TraPPE-UA force field.

Another important point for this work is the computational performance of the AUA4 force field compared to all-atom force fields. Figure 10 shows a comparison of the computational performance in the 3 molecules simulation with the AUA4 force field and the OPLS force field. The conditions of this simulation are a box with 1000 molecules at ambient conditions and all the simulation details described in the Henry's law constant calculation section.

It can be observed that in all cases there is a significant gain in computational performance. This gain depends on each molecule because each AUA4 force field molecule is represented with a number of different virtual sites and atomic sites and these are the main factor in determining the computational cost.

Figure 10 – Computational performance of the AUA4 in comparison with OPLS force field.

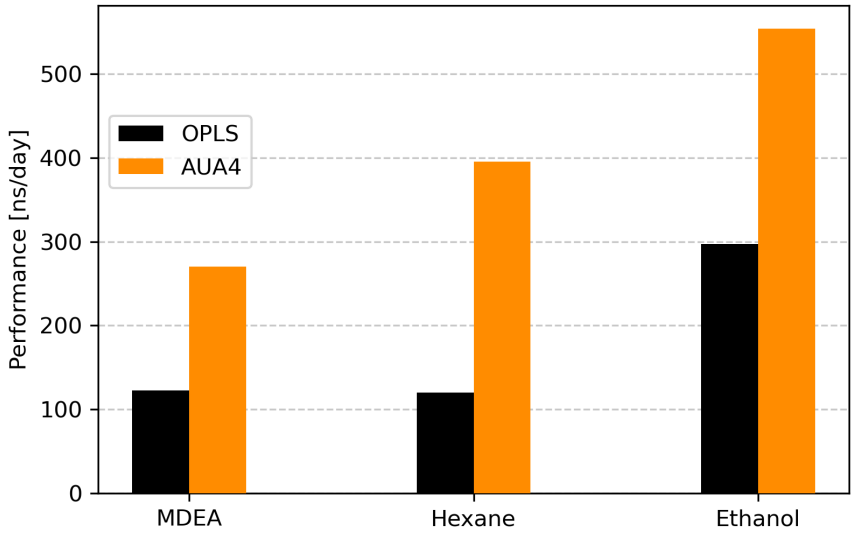

Source: The author.

Roughly speaking, it can be said that using the AUA4 force field there is a gain of a factor of 2 in computational time in conjunction with an accuracy in the reproduction of properties equal or superior to similar force fields.

4.3 OPTIMIZED INTERMOLECULAR POTENTIAL

Figures 11-13 show the result for each of the stages of the optimization process.The optimized parameters are present in table 8 along with the parameters obtained from the Lorentz Berthelot combining rule. In all cases there is a palpable improvement in the reproduction of the excess properties. In all cases the intermolecular potential correctly predicted the general behavior of the excess properties, however quantitatively the intermolecular potential underestimates the magnitude of the ideal mixture deviation. It is also notable that, in the sequence of optimizations, the mixture of ethanol and carbon dioxide hardly required any adjustments, which is an indication that the major deviation is in the interactions of the carbon dioxide oxygen atom with the primary carbon, adjusted during the first stage.

Although the percentage change in the lennard jones parameters does not appear to be very large, it has a large impact on the excess properties and, as will be seen in the next section also in the recreation of solubility. The magnitude of these changes corresponds well with that obtained in other studies where optimization of the inter-

Figure 11 – Experimental (green squares) and predicted excess enthalpy and excess volume for Ethane/CO2 with the cross interaction parameters using Lorentz-Berthelot combining rule (blue circles) and the optimized cross interaction parameters (orange circles).

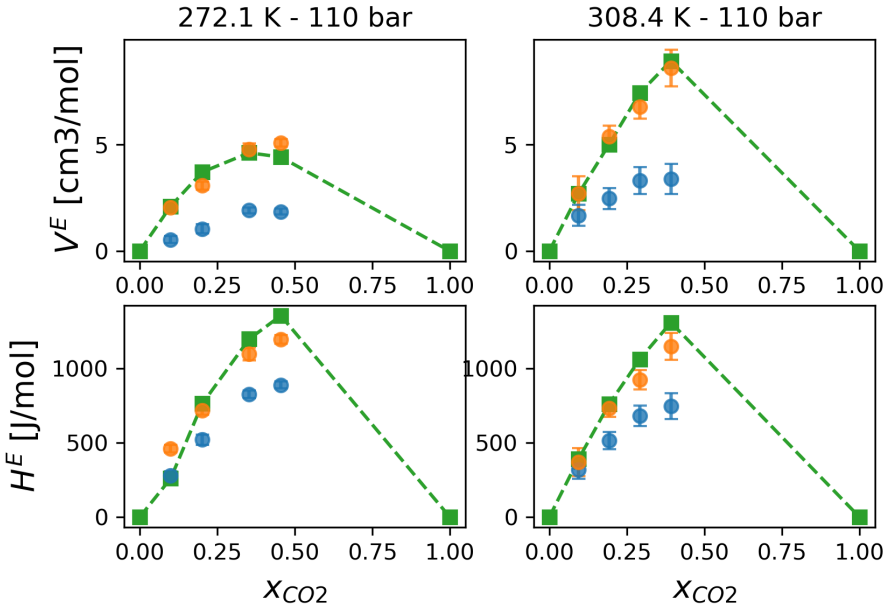

Source: The author.

molecular interaction parameters was performed. For example Kohns et al. (KOHNS et al., 2017) in the study of solubility of CO2 in ethanol scaled all the cross-energy lennard jones parameters ($\varepsilon_{i,j}$) in about +6%. Orozco et al. (OROZCO; ECONOMOU; PANAGIOTOPOULOS, 2014) in studying the phase equilibrium of water and carbon dioxide, found that the sigma parameter would require adjustments on the order of 2% while the epsilon parameter could be as large as +15%.

Table 8 – Original and optimized Lennard-Jones cross-interaction parameters along with the percentage of change.

Sitei	***Sitej***	σ_{ij}	ε_{ij}	$\sigma_{ij}^{Optimized}$	$\varepsilon_{ij}^{Optimized}$	**%Sigma**	**%Epsilon**
CH3	O(CO2)	0.3318	0.8170	0.34541	0.78122	4.1%	-4.4%
CH2	O(CO2)	0.3245	0.6924	0.31366	0.69741	-3.3%	0.7%
O(Alcohol)	O(CO2)	0.3055	0.8334	0.30537	0.82714	0.0%	-0.7%

Source: The author.

4.4 EVALUATION OF OPTIMIZED INTERMOLECULAR POTENTIAL

To evaluate the optimized model for use in the prediction of Henry's constant, this property was evaluated in the molecules used in the optimization process and

Figure 12 – Experimental (green squares) and predicted excess enthalpy and excess volume for hexane/CO2 with the cross interaction parameters using Lorentz-Berthelot combining rule (blue circles) and the optimized cross interaction parameters (orange circles).

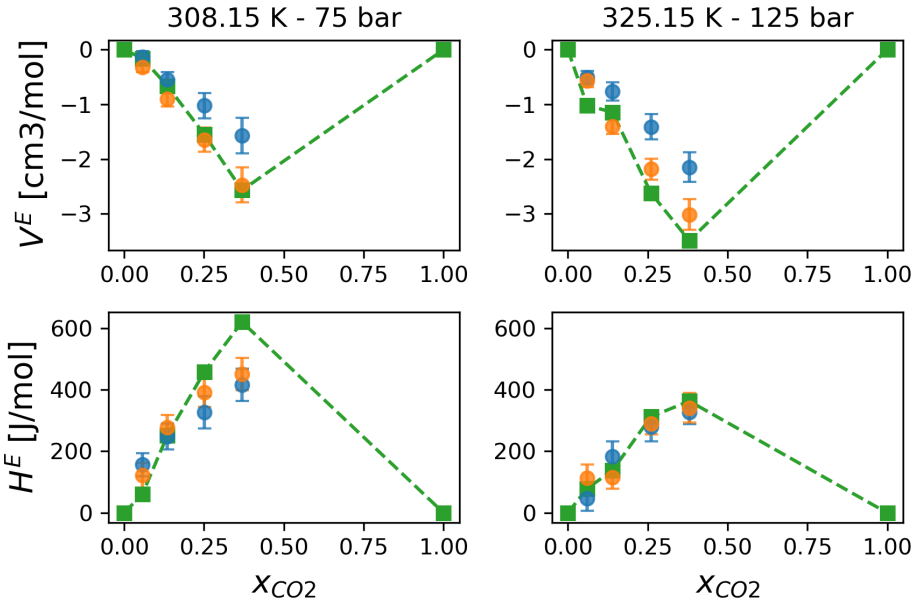

Source: The author.

the results were compared with the available experimental data. For the case of HEX, although the experimental information is not abundant, there seems to be agreement between the experimental data presented, however it is desirable to have more experimental data because the Henry's constant is a property with a high inherent systematic error. Thus, Figure 15 presents the predictions obtained with the original and the optimized potential. Where the latter improves solubility predictions by reducing the average error from 33.4% to 11.2%.

In the case of EtOH, there is a larger amount of data on CO2 solubility in this compound, being the study performed by Decultot et al. ((DÉCULTOT et al., 2019)) the one that covers a wider temperature range and whose behavior is very close to that of other studies. It is worth mentioning the data of Friend et al. (FRIEND et al., 2005) which belong to the second simulation challenge and are the ones rigorously measured and for which the uncertainty were reported. Figure 4 shows the predictions made with the original and optimized intermolecular potentials and the data published by Decultot et al., Friend et al. and Damlmolin et al. (DALMOLIN et al., 2006), which have been used in previous computational studies. A significant improvement is observed in the predictions using the optimized potential from a mean absolute deviation of 23.2% to 3.5%. Additionally optimized potential is able to be extrapolated (transferred) until

Figure 13 – Experimental (green squares) and predicted excess enthalpy and excess volume for Ethanol/CO2 with the cross interaction parameters using Lorentz-Berthelot combining rule (blue circles) and the optimized cross interaction parameters (orange circles).

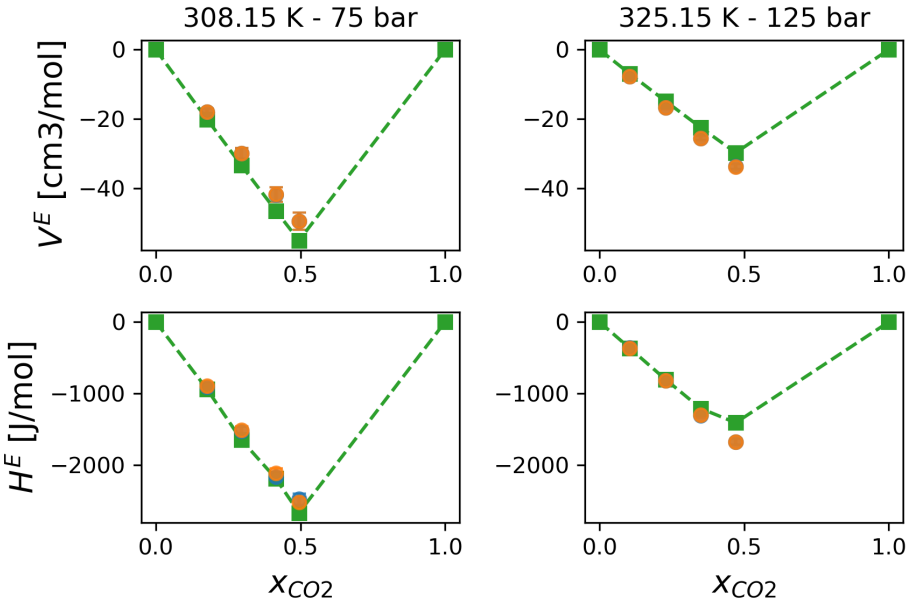

Source: The author.

temperatures as higher as 373.15 K, this is notably considering that the optimization process was done with temperatures between 308.15 and 325.15 K.

The tertiary amines TRE and NMM were also simulated, for these compounds only one experimental data of Henry's law constant was obtained. Of particular interest is TRE, this molecule contains only the CH3, CH2 and N3 groups, and its deviation was greatly reduced, passing from an overestimation of from +28.5% to +11.2%, without having been adjusted for the nitrogen interaction. On the other hand, predictions over NMM increased the deviation, passing from +3.7% to -14.1%. This deviation is in the order of magnitude of other deviations as can be seen in table 9. Additionally, this molecule contains an ether in its structure, so it ends up having two interactions that can be adjusted.

It is clear that the potential, although optimized in supercritical conditions with excess properties, greatly improves the predictions of Henry's law constant, without falling into the direct optimization on this property, which is much more computationally intensive and also has a relatively higher systematic error than the measurement and calculation of excess properties. The success of this optimization procedure lies in the fact that the excess enthalpy and excess volume are the derivatives of the excess chemical potential with respect to temperature and pressure respectively, as expressed by

Figure 14 – Carbon dioxide solubility predictions in HEX with the original potential (blue triangles) and with the optimized potential (orange circles). The solid black line corresponds to the correlation available for HEX (LORIMER; CLEVER; YOUNG, 1992), the dashed black corresponds to the extrapolation of such correlation.

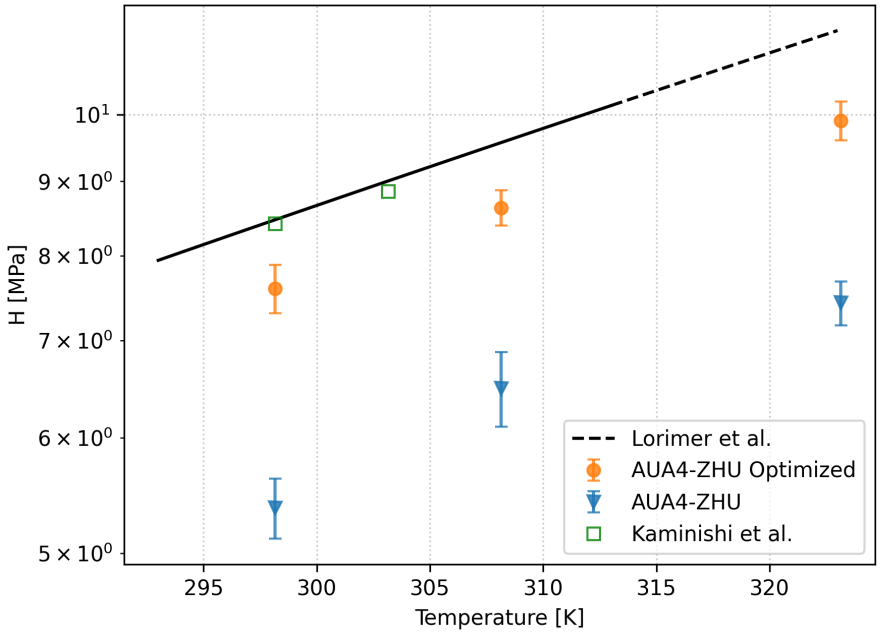

Source: The author.

Table 9 – Deviations from the original and optimized intermolecular potentials.

Molecule	**T [K]**	**%AAD**	**%AAD optmized**
HEX	298.15 - 323.15	33.4%	11.2%
EtOH	293.15 - 373.15	23.2%	3.5%
TRE	298.15	28.7%	11.2%
NMM	298.15	3.7%	14.1%
Average	-	22.3%	10.0%

Source: The author.

the 4.4. Furthermore, the excess enthalpy and excess volume actually reflect how the binary interactions depart from the behavior of the pure substance, so it makes sense to adjust the cross intermolecular interaction parameteres with this pair of properties. In fact, Jaubert et al. (JAUBERT et al., 2022) showed that the use of excess enthalpy and excess specific heat in the optimization of binary interaction parameters greatly increases the predictive power of the Peng Robinson-based equation of state. Similarly, Brouwer et al. (BROUWER et al., 2023) recently showed that the parameterization

Figure 15 – Carbon dioxide solubility predictions in EtOH with the original potential (blue triangles) and with the optimized potential (orange circles). The squares represent experimental data from the works of (DALMOLIN et al., 2006) (red), (FRIEND et al., 2005) (black) and (DÉCULTOT et al., 2019) (green).

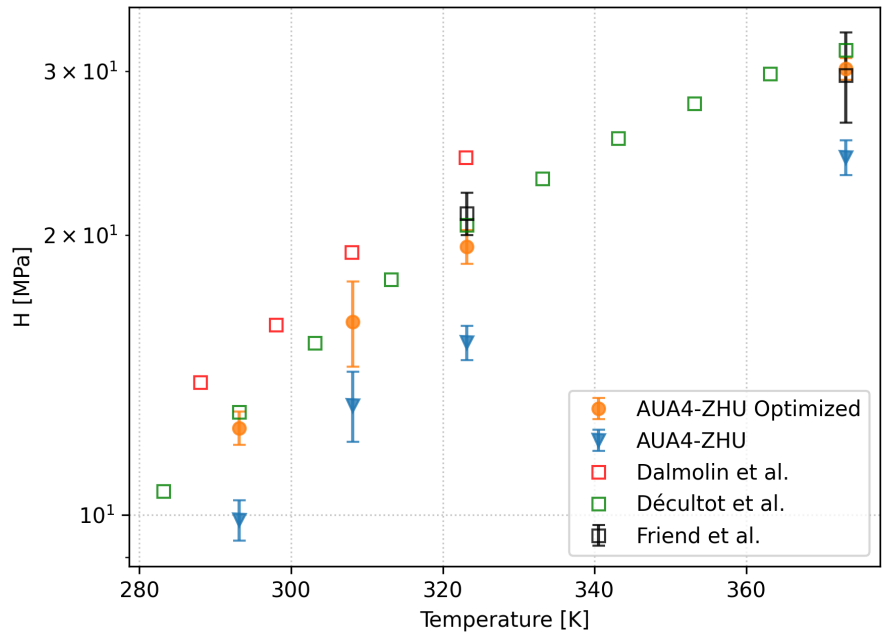

Source: The author.

of the SAFT equation of state using excess enthalpy data was particularly useful for the study of vapor-liquid equilibrium of highly non-ideal mixtures. Regarding the supercritical conditions worked out in the optimization procedure, these were selected, as much as possible, in such a way as to approximate the conditions at which the carbon dioxide would be found dissolved in a solvent during absorption process, i.e. at near ambient temperatures and densities of liquid organic substances. Or from a molecular perspective, the optimization conditions resemble the evaluation conditions in terms of the thermal energy experienced by the molecules and the molecular distances between atomic sites.

$$\left(\frac{\partial(\mu_i^{excess}/RT)}{\partial P}\right)_{T,x_i} = \frac{\overline{V}_{m,i}{}^{excess}}{RT} \tag{30a}$$

$$\left(\frac{\partial(\mu_i^{excess}/RT)}{\partial T}\right)_{P,x_i} = -\frac{\overline{h}_i^{excess}}{RT^2} \tag{30b}$$

It is worth noting that optimization over excess properties is more convenient from the computational performance point of view because these properties have in general lower computational uncertainty and simulation times are much shorter than simulations employed in free energy calculations.

Having discussed this, we applied the optimized potential to study the behavior of CO2 solubility in tertiary alkanolamines, namely MDEA and TEA. Figure 16 presents the Henry's law constant predictions with the optimized potential as well as the previously analyzed experimental data. Additionally, we plotted the solubility predicted by the N2O analogy, using CO2 and N2O correlations for Henry law in water presented in Monteiro et al. (MONTEIRO; SVENDSEN, 2015), the experimental measurements of N2O solubility reported in Wange et al. (WANG, Y. W. et al., 1992) and the equation (3). While there are discrepancies between the simulated data and the experimental data at low temperatures, these differences are due in part to the non-optimized amine tertiary group and also could be explained by some residual chemical reaction, which can largely mask the true physical solubility, as seen in the case of DMEA. The latter explains why the experimental data and our predictions get closer at higher temperatures. Although the N2O analogy is only generally valid in a dilute solution of amines and not in pure amines, in this case the results of the optimized potential and those of the analogy agree in the temperature range.

As a counterpoint, Figure 17 shows the predictions of Henry's constant with the optimized potential for TEA. As can be seen in this case there is a large discrepancy between the two predictions. For this molecule, as shown in the analysis of the experimental data, the chemical solubility data has indications of being affected by some chemical reaction and therefore could not be calculated according to Henry's law or presented here.

4.5 LIMITATIONS

While our optimized potential has shown promising results, it is essential to acknowledge some inherent limitations. First and foremost, the optimization problem was reduced by taking just the interactions with the oxygen atoms of the carbon dioxide molecule leaving aside the interactions with the carbon atom of the carbon dioxide molecule. In addition, we are aware that the number of experimental data is limited and a more robust optimization process must include a larger number of molecules and conditions. Furthermore, the sequential and transfer optimization process, while saving computational time, arrives at a set of parameters that does not necessarily reach the global minimum. An alternative is a global optimization process that includes a larger number of substances and several initial points. Finally, we would like to point out that an optimal parameter set, satisfying the above mentioned constraints, will be subject to the intrinsic limitations of the force fields (AUA4 and ZHU in this study) to recreate the

Figure 16 – Carbon dioxide solubility predictions in MDEA with the optimized potential (orange circles). The squares correspond to experimental data from the works of Skylogianni et al. (SKYLOGIANNI et al., 2020) (green). Red triangles represent data computed with N2O analogy.

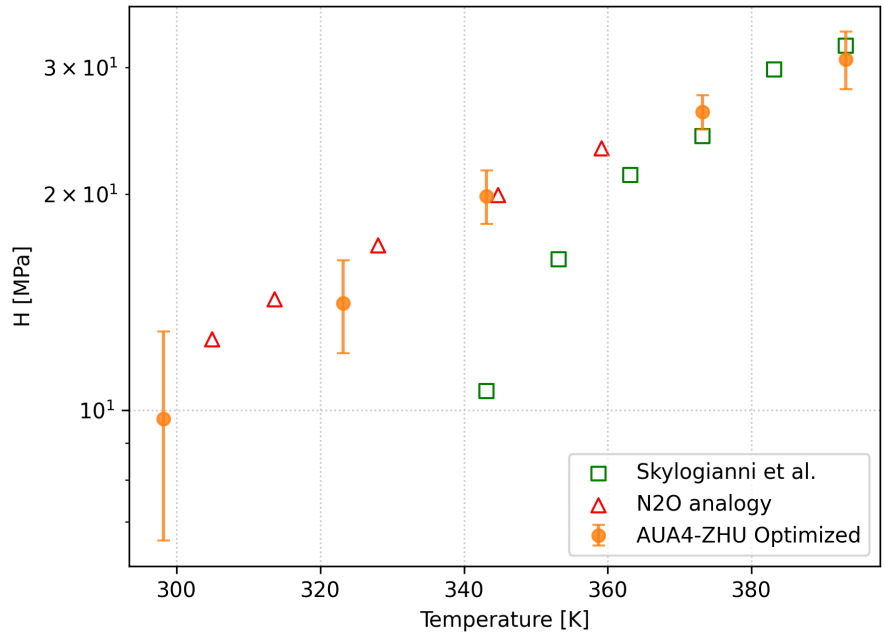

Source: The author.

behavior of the substances.

Figure 17 – Carbon dioxide solubility predictions in TEA with the optimized potential (orange circles). Red triangles represent data computed with N2O analogy.

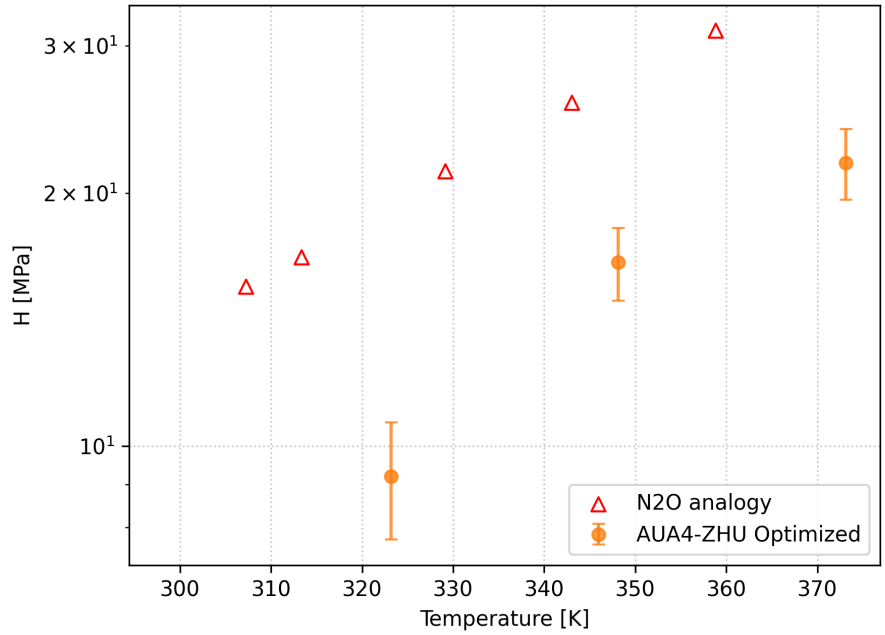

Source: The author.

5 CONCLUSIONS

In the context of carbon dioxide capture by solvents, the problem of choosing wisely among the vast chemical solvent space available arises. To bridge this gap using state-of-art computational techniques, in this work we propose the optimization of the intermolecular cross interactions of a force field focused on the prediction of the physical solubility of CO2 in tertiary amines and alkanolamines. Based on this objective and those ones presented on the introduction we conclude that:

a) A detailed analysis of the available experimental data for tertiary amines and tertiary alkanolamines indicates the possible presence of chemical reactions in the latter. The extension of the reaction seems to decrease with temperature and masks the physical solubility by up to a factor of 4. This distinction between physical and chemical solubility is an essential step for the selection of the experimental data used in the optimization and assessment of intermolecular potential.

b) The AUA4 model was successfully implemented and validated for the study of equilibrium properties of organic substances, in which the accuracy was equal or superior to that of other models of similar physical detail and proved to provide computational efficiency twice that of all-atom models. This was of great value due to the high computational cost of the simulations used to calculate Henry's law constant.

c) The ability to use excess enthalpy and excess volume data to improve the prediction of physical solubility was demonstrated. A set of 6 intermolecular cross-interaction parameters corresponding to the sigma and epsilon values of the atom sites forming any linear alcohol: alcohols and linear alkanes, could be inexpensively optimized by means of an optimization and transfer scheme. The corrections found were lower or equal to similar works that perform the optimization of these molecular parameters. The most significant adjustment was over the terminal carbon and oxygen carbon dioxide atom.

d) The optimized intermolecular potential significantly improved the predictions of the Henry's law constant in the molecules used in the optimization process. It also ensured that the behavior with temperature was correctly reproduced even at temperatures higher than those contemplated in the optimization process. The optimized intermolecular potential also showed signs of improving solubility prediction in tertiary amines, in the case of TRE it reduced the deviation from 24%AAD to just over 11%AAD. Overall, there was an error reduction from 22.3%AAD to 10.0%AAD.

e) The optimized intermolecular potential predictions on the tertiary alkanolamine

MDEA showed that at high temperatures there is a correspondence between the data predicted by the model and the experimental data, while at low temperatures there are insufficient experimental data and those that exist are probably influenced by chemical solubility of CO2.

5.1 FUTURE PROSPECTS

The result of this work is an optimized intermolecular potential capable of recreating the Henry's law behavior in amines and alkanolamines with moderate deviations. It also highlights the novelty in the methodology of optimizing the intermolecular parameters with excess properties. For these two reasons this work can be a fundamental piece for future research:

a) The extension of the model and application in aqueous mixtures, in which the carbonate formation reaction is important. The model can be coupled with other phenomenological models or with experimental results to reveal the kinetics and mass transfer phenomena, due to Henry's constant is an indispensable parameter for the description of the rate of mass transfer and reaction.

b) The use of the model in solvent mixtures to study the behavior of solubility and other properties related to the energetic performance of solvents for carbon dioxide capture, based on synergy effects, would be a promising area.

c) The AUA4 force field and ZHU force field used here are remarkable for their ability to predict the transport properties of pure substances better than other models of a similar level of complexity. A next step would be the evaluation of this optimized intermolecular potential for the study of transport properties related to the absorption of carbon dioxide such as the viscosity of carbon dioxide loaded solutions and the intrinsic diffusion coefficient of carbon dioxide.

d) A study with experimental data of supercritical mixtures of tertiary amines and carbon dioxide would allow the adjustment of the cross-interaction between the nitrogen of the tertiary amine and carbon dioxide, in conjunction with carbon dioxide adsorption isotherms in this kind of substances, to obtain a more robust optimization of the intermolecular potential.

REFERENCES

ABRAHAM, Mark James; MURTOLA, Teemu; SCHULZ, Roland; PÁLL, Szilárd; SMITH, Jeremy C.; HESS, Berk; LINDAHL, Erik. GROMACS: High performance molecular simulations through multi-level parallelism from laptops to supercomputers. en. **SoftwareX**, v. 1-2, p. 19–25, Sept. 2015. ISSN 2352-7110.

ABU-ARABI, Mousa K.; AL-JARRAH, Asem M.; EL-EIDEH, Mohammed; TAMIMI, A. Physical Solubility and Diffusivity of CO2 in Aqueous Diethanolamine Solutions. **J. Chem. Eng. Data**, v. 46, n. 3, p. 516–521, May 2001. Publisher: American Chemical Society. ISSN 0021-9568.

AHUNBAY, M. Göktuğ; PEREZ-PELLITERO, Javier; CONTRERAS-CAMACHO, R. Oliver; TEULER, Jean-Marie; UNGERER, Philippe; MACKIE, Allan D.; LACHET, Véronique. Optimized Intermolecular Potential for Aromatic Hydrocarbons Based on Anisotropic United Atoms. III. Polyaromatic and Naphthenoaromatic Hydrocarbons. **J. Phys. Chem. B**, v. 109, n. 7, p. 2970–2976, Feb. 2005. Publisher: American Chemical Society. ISSN 1520-6106.

AIDA, Tsutomu; AIZAWA, Takafumi; KANAKUBO, Mitsuhiro; NANJO, Hiroshi. Relation between Volume Expansion and Hydrogen Bond Networks for CO2Alcohol Mixtures at 40 ℃. **J. Phys. Chem. B**, v. 114, n. 43, p. 13628–13636, Nov. 2010. Publisher: American Chemical Society. ISSN 1520-6106.

ALAVI, Saman. **Molecular Simulations: Fundamentals and Practice**. [S.l.]: WILEY VCH. ISBN 978-3-527-69953-7.

ALLEN, Michael P.; TIDESLEY, Dominic J. Some tricks of the trade. In: COMPUTER Simulation of Liquids. Second Edition. [S.l.]: Oxford University Press. ISBN 978-0-19-880320-1.

AQUING, Michelle et al. Composition Analysis and Viscosity Prediction of Complex Fuel Mixtures Using a Molecular-Based Approach. **Energy Fuels**, v. 26, n. 4, p. 2220–2230, Apr. 2012. Publisher: American Chemical Society. ISSN 0887-0624.

ARRIOLA GONZÁLEZ, Kevin R; ARMAS-PEREZ, Julio C; VÁZQUEZ-NÚÑEZ, Edgar; CÁRDENAS, José Carlos; MENDOZA, Angeles; REYES-AGUILERA, José Antonio; FIGUEROA-GERSTENMAIER, Susana. Determination of liquid–vapor equilibrium and critical properties of fatty acids for biodiesel production through molecular dynamics.

en. **J. Phys.: Condens. Matter**, v. 34, n. 21, p. 214002, May 2022. ISSN 0953-8984, 1361-648X.

ASSOCIAÇÃO BRASILEIRA DE NORMAS TÉCNICAS. **NBR 10520**: Informação e documentação — Citações em documentos — Apresentação. Rio de Janeiro, Aug. 2002.

ASSOCIAÇÃO BRASILEIRA DE NORMAS TÉCNICAS. **NBR 6023**: Informação e documentação — Referências — Apresentação. Rio de Janeiro, Aug. 2002.

ASSOCIAÇÃO BRASILEIRA DE NORMAS TÉCNICAS. **NBR 6027**: Informação e documentação — Sumário — Apresentação. Rio de Janeiro, Dec. 2012.

ASSOCIAÇÃO BRASILEIRA DE NORMAS TÉCNICAS. **NBR 6028**: Informação e documentação — Resumo — Apresentação. Rio de Janeiro, Nov. 2003.

BALCHANDANI, Sweta; SINGH, Ramesh. COSMO-RS Analysis of CO2 Solubility in N-Methyldiethanolamine, Sulfolane, and 1-Butyl-3-methyl-imidazolium Acetate Activated by 2-Methylpiperazine for Postcombustion Carbon Capture. **ACS Omega**, v. 6, n. 1, p. 747–761, Jan. 2021. Publisher: American Chemical Society.

BALCHANDANI, Sweta C; MANDAL, Bishnupada; DHARASKAR, Swapnil. Stimulation of CO2 solubility in reversible ionic liquids activated by novel 1-(2-aminoethyl piperazine) and bis (3-aminopropyl) amine. **Separation and Purification Technology**, v. 262, p. 118260, May 2021. ISSN 1383-5866.

BEHRENS, Richard; HARBOU, Erik von; THIEL, Werner R.; BÖTTINGER, Wolfram; INGRAM, Thomas; SIEDER, Georg; HASSE, Hans. Monoalkylcarbonate Formation in Methyldiethanolamine–H2O–CO2. **Ind. Eng. Chem. Res.**, v. 56, n. 31, p. 9006–9015, Aug. 2017. Publisher: American Chemical Society. ISSN 0888-5885.

BEHRENS, Richard; KESSLER, Elmar; MÜNNEMANN, Kerstin; HASSE, Hans; HARBOU, Erik von. Monoalkylcarbonate formation in the system monoethanolamine–water–carbon dioxide. **Fluid Phase Equilibria**, v. 486, p. 98–105, May 2019. ISSN 0378-3812.

BOURASSEAU, Emeric; HABOUDOU, Mehalia; BOUTIN, Anne; FUCHS, Alain H.; UNGERER, Philippe. New optimization method for intermolecular potentials: Optimization of a new anisotropic united atoms potential for olefins: Prediction of

equilibrium properties. **J. Chem. Phys.**, v. 118, n. 7, p. 3020–3034, Feb. 2003. Publisher: American Institute of Physics. ISSN 0021-9606.

BOURASSEAU, Emeric; UNGERER, Philippe; BOUTIN, Anne. Prediction of Equilibrium Properties of Cyclic Alkanes by Monte Carlo SimulationNew Anisotropic United Atoms Intermolecular PotentialNew Transfer Bias Method. en. **J. Phys. Chem. B**, v. 106, n. 21, p. 5483–5491, May 2002. ISSN 1520-6106, 1520-5207.

BOURASSEAU, Emeric; UNGERER, Philippe; BOUTIN, Anne; FUCHS, Alain H. Monte Carlo simulation of branched alkanes and long chain n -alkanes with anisotropic united atoms intermolecular potential. **Molecular Simulation**, v. 28, n. 4, p. 317–336, Apr. 2002. Publisher: Taylor & Francis _eprint: https://doi.org/10.1080/08927020290018723. ISSN 0892-7022.

BROUWER, Thomas; CRESPO, Emanuel A.; KATE, Antoon ten; COUTINHO, João A. P.; KERSTEN, Sascha R. A.; BARGEMAN, Gerrald; SCHUUR, Boelo. Isobaric Vapor–Liquid Equilibrium Prediction from Excess Molar Enthalpy Using Cubic Equations of State and PC-SAFT. **Ind. Eng. Chem. Res.**, v. 62, n. 31, p. 12329–12344, Aug. 2023. Publisher: American Chemical Society. ISSN 0888-5885.

BUDHATHOKI, Samir; SHAH, Jindal K.; MAGINN, Edward J. Molecular Simulation Study of the Solubility, Diffusivity and Permselectivity of Pure and Binary Mixtures of CO2 and CH4 in the Ionic Liquid 1-n-Butyl-3-methylimidazolium bis(trifluoromethylsulfonyl)imide. **Ind. Eng. Chem. Res.**, v. 54, n. 35, p. 8821–8828, Sept. 2015. Publisher: American Chemical Society. ISSN 0888-5885.

CANTU, David C.; LEE, Juntaek; LEE, Mal-Soon; HELDEBRANT, David J.; KOECH, Phillip K.; FREEMAN, Charles J.; ROUSSEAU, Roger; GLEZAKOU, Vassiliki-Alexandra. Dynamic Acid/Base Equilibrium in Single Component Switchable Ionic Liquids and Consequences on Viscosity. **J. Phys. Chem. Lett.**, v. 7, n. 9, p. 1646–1652, May 2016. Publisher: American Chemical Society.

CAO, Hengguang; CAO, Xuewen; CHEN, Junwen; ZHAO, Xiangyang; DING, Gaoya; GUO, Dan; LIU, Yang; LI, Hao; BIAN, Jiang. Molecular dynamics simulation of the transport properties and condensation mechanism of carbon dioxide. **Journal of Natural Gas Science and Engineering**, v. 105, p. 104692, Sept. 2022. ISSN 1875-5100.

CASTRO ANAYA, Luis Eduardo; GÓMEZ, Sergio Y.; OROZCO, Gustavo A. Comprehensive Automated Routine Implementation, Validation, and Benchmark of the Anisotropic Force Field (AUA4) Using Python and GROMACS. **J. Phys. Chem. A**, v. 127, n. 6, p. 1555–1563, Feb. 2023. Publisher: American Chemical Society. ISSN 1089-5639.

CHEN, Qu; BALAJI, Sayee Prasaad; RAMDIN, Mahinder; GUTIÉRREZ-SEVILLANO, Juan José; BARDOW, André; GOETHEER, Earl; VLUGT, Thijs J. H. Validation of the CO2/N2O Analogy Using Molecular Simulation. **Ind. Eng. Chem. Res.**, v. 53, n. 46, p. 18081–18090, Nov. 2014. Publisher: American Chemical Society. ISSN 0888-5885.

CHEN, Qu; RAMDIN, Mahinder; VLUGT, Thijs J. H. Solubilities of CO2, CH4, C2H6, CO, H2, N2, N2O, and H2S in commercial physical solvents from Monte Carlo simulations. **Molecular Simulation**, v. 49, n. 13-14, p. 1341–1349, Sept. 2023. Publisher: Taylor & Francis _eprint: https://doi.org/10.1080/08927022.2023.2228918. ISSN 0892-7022.

CHOWDHURY, Firoz Alam; YAMADA, Hidetaka; HIGASHII, Takayuki; GOTO, Kazuya; ONODA, Masami. CO2 Capture by Tertiary Amine Absorbents: A Performance Comparison Study. **Ind. Eng. Chem. Res.**, v. 52, n. 24, p. 8323–8331, June 2013. Publisher: American Chemical Society. ISSN 0888-5885.

CIESLAROVA, Zuzana; SANTOS, Vagner Bezerra dos; LAGO, Claudimir Lucio do. Both carbamates and monoalkyl carbonates are involved in carbon dioxide capture by alkanolamines. **International Journal of Greenhouse Gas Control**, v. 76, p. 142–149, Sept. 2018. ISSN 1750-5836.

CONTRERAS-CAMACHO, R. Oliver; UNGERER, Philippe; AHUNBAY, M. Goktug; LACHET, Véronique; PEREZ-PELLITERO, Javier; MACKIE, Allan D. Optimized Intermolecular Potential for Aromatic Hydrocarbons Based on Anisotropic United Atoms. 2. Alkylbenzenes and Styrene. **J. Phys. Chem. B**, v. 108, n. 37, p. 14115–14123, Sept. 2004. Publisher: American Chemical Society. ISSN 1520-6106.

CONTRERAS-CAMACHO, R. Oliver; UNGERER, Philippe; BOUTIN, Anne; MACKIE, Allan D. Optimized Intermolecular Potential for Aromatic Hydrocarbons Based on Anisotropic United Atoms. 1. Benzene. **J. Phys. Chem. B**, v. 108, n. 37, p. 14109–14114, Sept. 2004. Publisher: American Chemical Society. ISSN 1520-6106.

CORDRAY, D. R.; IZATT, R. M.; CHRISTENSEN, J. J.; OSCARSON, J. L. The excess enthalpies of (carbon dioxide + ethanol) at 308.15, 325.15, 373.15, 413.15, and 473.15 K from 5.00 to 14.91 MPa. **The Journal of Chemical Thermodynamics**, v. 20, n. 6, p. 655–663, June 1988. ISSN 0021-9614.

CUNICO, Larissa P.; TURNER, Charlotta. Density Measurements of CO2-Expanded Liquids. **J. Chem. Eng. Data**, v. 62, n. 10, p. 3525–3533, Oct. 2017. Publisher: American Chemical Society. ISSN 0021-9568.

DALMOLIN, I.; SKOVROINSKI, E.; BIASI, A.; CORAZZA, M. L.; DARIVA, C.; OLIVEIRA, J. Vladimir. Solubility of carbon dioxide in binary and ternary mixtures with ethanol and water. **Fluid Phase Equilibria**, v. 245, n. 2, p. 193–200, Aug. 2006. ISSN 0378-3812.

DAWASS, Noura; WANDERLEY, Ricardo R.; RAMDIN, Mahinder; MOULTOS, Othonas A.; KNUUTILA, Hanna K.; VLUGT, Thijs J. H. Solubility of Carbon Dioxide, Hydrogen Sulfide, Methane, and Nitrogen in Monoethylene Glycol; Experiments and Molecular Simulation. **J. Chem. Eng. Data**, v. 66, n. 1, p. 524–534, Jan. 2021. Publisher: American Chemical Society. ISSN 0021-9568.

DÉCULTOT, Marie; LEDOUX, Alain; FOURNIER-SALAÜN, Marie-Christine; ESTEL, Lionel. Solubility of CO2 in methanol, ethanol, 1,2-propanediol and glycerol from 283.15K to 373.15K and up to 6.0MPa. **The Journal of Chemical Thermodynamics**, v. 138, p. 67–77, Nov. 2019. ISSN 0021-9614.

DUTCHER, Bryce; FAN, Maohong; RUSSELL, Armistead G. Amine-Based CO2 Capture Technology Development from the Beginning of 2013—A Review. **ACS Appl. Mater. Interfaces**, v. 7, n. 4, p. 2137–2148, Feb. 2015. Publisher: American Chemical Society. ISSN 1944-8244.

EDWARDS, T. J.; MAURER, Gerd; NEWMAN, John; PRAUSNITZ, J. M. Vapor-liquid equilibria in multicomponent aqueous solutions of volatile weak electrolytes. en. **AIChE Journal**, v. 24, n. 6, p. 966–976, 1978. _eprint: https://onlinelibrary.wiley.com/doi/pdf/10.1002/aic.690240605. ISSN 1547-5905.

AL-FAZARI, Fatma R.; MJALLI, Farouq S.; SHAKOURIAN-FARD, Mehdi; KAMATH, Ganesh; NASER, Jamil; MURSHID, Ghulam; AL MA'AWALI, Suhaib. Imidazole–Monoethanolamine-Based Deep Eutectic Solvent for Carbon Dioxide Capture: A Combined Experimental and Molecular Dynamics Investigation. **J. Chem.**

Eng. Data, v. 68, n. 5, p. 1077–1090, May 2023. Publisher: American Chemical Society. ISSN 0021-9568.

FERRANDO, Nicolas; GEDIK, Ibrahim; LACHET, Véronique; PIGEON, Laurent; LUGO, Rafael. Prediction of Phase Equilibrium and Hydration Free Energy of Carboxylic Acids by Monte Carlo Simulations. **J. Phys. Chem. B**, v. 117, n. 23, p. 7123–7132, June 2013. Publisher: American Chemical Society. ISSN 1520-6106.

FERRANDO, Nicolas; LACHET, Véronique; BOUTIN, Anne. Monte Carlo Simulations of Mixtures Involving Ketones and Aldehydes by a Direct Bubble Pressure Calculation. **J. Phys. Chem. B**, v. 114, n. 26, p. 8680–8688, July 2010. Publisher: American Chemical Society. ISSN 1520-6106.

FERRANDO, Nicolas; LACHET, Véronique; BOUTIN, Anne. Transferable Force Field for Carboxylate Esters: Application to Fatty Acid Methylic Ester Phase Equilibria Prediction. **J. Phys. Chem. B**, v. 116, n. 10, p. 3239–3248, Mar. 2012. Publisher: American Chemical Society. ISSN 1520-6106.

FERRANDO, Nicolas; LACHET, Véronique; PÉREZ-PELLITERO, Javier; MACKIE, Allan D.; MALFREYT, Patrice; BOUTIN, Anne. A Transferable Force Field To Predict Phase Equilibria and Surface Tension of Ethers and Glycol Ethers. **J. Phys. Chem. B**, v. 115, n. 36, p. 10654–10664, Sept. 2011. Publisher: American Chemical Society. ISSN 1520-6106.

FERRANDO, Nicolas; LACHET, Véronique; TEULER, Jean-Marie; BOUTIN, Anne. Transferable Force Field for Alcohols and Polyalcohols. **J. Phys. Chem. B**, v. 113, n. 17, p. 5985–5995, Apr. 2009. Publisher: American Chemical Society. ISSN 1520-6106.

FISCHER, Nina M.; MAAREN, Paul J. van; DITZ, Jonas C.; YILDIRIM, Ahmet; SPOEL, David van der. Properties of Organic Liquids when Simulated with Long-Range Lennard-Jones Interactions. **J. Chem. Theory Comput.**, v. 11, n. 7, p. 2938–2944, July 2015. Publisher: American Chemical Society. ISSN 1549-9618.

FRIEND, Daniel G.; FRURIP, David J.; LEMMON, Eric W.; MORRISON, Richard E.; OLSON, James D.; WILSON, Loren C. Establishing benchmarks for the Second Industrial Fluids Simulation Challenge. **Fluid Phase Equilibria**, v. 236, n. 1, p. 15–24, Sept. 2005. ISSN 0378-3812.

GANGARAPU, Satesh; MARCELIS, Antonius T. M.; ZUILHOF, Han. Carbamate Stabilities of Sterically Hindered Amines from Quantum Chemical Methods: Relevance for CO2 Capture. en. **ChemPhysChem**, v. 14, n. 17, p. 3936–3943, 2013. _eprint: https://onlinelibrary.wiley.com/doi/pdf/10.1002/cphc.201300820. ISSN 1439-7641.

GONZÁLEZ, M. A. Force fields and molecular dynamics simulations. en. **JDN**, v. 12, p. 169–200, 2011. Publisher: EDP Sciences. ISSN 2107-7223, 2107-7231.

GONZALEZ-MIQUEL, Maria et al. COSMO-RS Studies: Structure–Property Relationships for CO2 Capture by Reversible Ionic Liquids. **Ind. Eng. Chem. Res.**, v. 51, n. 49, p. 16066–16073, Dec. 2012. Publisher: American Chemical Society. ISSN 0888-5885.

JAUBERT, Jean-Noël; QIAN, Jun-Wei; LASALA, Silvia; PRIVAT, Romain. The impressive impact of including enthalpy and heat capacity of mixing data when parameterising equations of state. Application to the development of the E-PPR78 (Enhanced-Predictive-Peng-Robinson-78) model. **Fluid Phase Equilibria**, v. 560, p. 113456, Sept. 2022. ISSN 0378-3812.

JOU, Fang-Yuan; MATHER, Alan E. Solubility of carbon dioxide in anhydrous triethanolamine. en. **The Canadian Journal of Chemical Engineering**, v. 101, n. 1, p. 474–476, 2023. _eprint: https://onlinelibrary.wiley.com/doi/pdf/10.1002/cjce.24530. ISSN 1939-019X.

JUNG, Wonho; LEE, Myungsuk; HWANG, Gyeong S.; KIM, Eunseok; LEE, Kwang Soon. Thermodynamic modeling and energy analysis of a polyamine-based water-lean solvent for CO2 capture. **Chemical Engineering Journal**, v. 399, p. 125714, Nov. 2020. ISSN 1385-8947.

KAPOOR, Utkarsh; SHAH, Jindal K. Molecular Origins of the Apparent Ideal CO2 Solubilities in Binary Ionic Liquid Mixtures. **J. Phys. Chem. B**, v. 122, n. 42, p. 9763–9774, Oct. 2018. Publisher: American Chemical Society. ISSN 1520-6106.

KIERZKOWSKA-PAWLAK, Hanna; ZARZYCKI, Roman. Solubility of Carbon Dioxide and Nitrous Oxide in Water + Methyldiethanolamine and Ethanol + Methyldiethanolamine Solutions. **J. Chem. Eng. Data**, v. 47, n. 6, p. 1506–1509, Nov. 2002. Publisher: American Chemical Society. ISSN 0021-9568.

KOHNS, Maximilian; WERTH, Stephan; HORSCH, Martin; HARBOU, Erik von; HASSE, Hans. Molecular simulation study of the CO2-N2O analogy. **Fluid Phase Equilibria**, v. 442, p. 44–52, June 2017. ISSN 0378-3812.

KORTUNOV, Pavel V.; SISKIN, Michael; PACCAGNINI, Michele; THOMANN, Hans. CO2 Reaction Mechanisms with Hindered Alkanolamines: Control and Promotion of Reaction Pathways. **Energy Fuels**, v. 30, n. 2, p. 1223–1236, Feb. 2016. Publisher: American Chemical Society. ISSN 0887-0624.

LADDHA, S. S.; DIAZ, J. M.; DANCKWERTS, P. V. The N2O analogy: The solubilities of CO2 and N2O in aqueous solutions of organic compounds. **Chemical Engineering Science**, v. 36, n. 1, p. 228–229, Jan. 1981. ISSN 0009-2509.

LEMAOUI, Tarek; BOUBLIA, Abir; LEMAOUI, Soumaya; DARWISH, Ahmad S.; ERNST, Barbara; ALAM, Manawwer; BENGUERBA, Yacine; BANAT, Fawzi; ALNASHEF, Inas M. Predicting the CO2 Capture Capability of Deep Eutectic Solvents and Screening over 1000 of their Combinations Using Machine Learning. **ACS Sustainable Chem. Eng.**, v. 11, n. 26, p. 9564–9580, July 2023. Publisher: American Chemical Society.

LEPAUMIER, Helene; MARTIN, Sandrine; PICQ, Dominique; DELFORT, Bruno; CARRETTE, Pierre-Louis. New Amines for CO2 Capture. III. Effect of Alkyl Chain Length between Amine Functions on Polyamines Degradation. **Ind. Eng. Chem. Res.**, v. 49, n. 10, p. 4553–4560, May 2010. Publisher: American Chemical Society. ISSN 0888-5885.

LEPAUMIER, Helene; PICQ, Dominique; CARRETTE, Pierre-Louis. New Amines for CO2 Capture. I. Mechanisms of Amine Degradation in the Presence of CO2. **Ind. Eng. Chem. Res.**, v. 48, n. 20, p. 9061–9067, Oct. 2009. Publisher: American Chemical Society. ISSN 0888-5885.

LI, Xiaoshan; LIU, Ji; JIANG, Wufeng; GAO, Ge; WU, Fan; LUO, Cong; ZHANG, Liqi. Low energy-consuming CO2 capture by phase change absorbents of amine/alcohol/H2O. **Separation and Purification Technology**, v. 275, p. 119181, Nov. 2021. ISSN 1383-5866.

LIU, Enbin; LU, Xudong; WANG, Daocheng. A Systematic Review of Carbon Capture, Utilization and Storage: Status, Progress and Challenges. en. **Energies**, v. 16, n. 6,

p. 2865, Jan. 2023. Number: 6 Publisher: Multidisciplinary Digital Publishing Institute. ISSN 1996-1073.

LIU, Sen; LING, Hao; GAO, Hongxia; TONTIWACHWUTHIKUL, Paitoon; LIANG, Zhiwu. Better Choice of Tertiary Alkanolamines for Postcombustion CO2 Capture: Structure with Linear Alkanol Chain Instead of Branched. **Ind. Eng. Chem. Res.**, v. 58, n. 33, p. 15344–15352, Aug. 2019. Publisher: American Chemical Society. ISSN 0888-5885.

LORIMER, J. W.; CLEVER, H. L.; YOUNG, C. L. **Carbon Dioxide in Non–Aqueous Solvents At Pressures Less Than 200 KPA**. [S.l.]: Elsevier, 1992. ISBN 978-0-08-040495-0.

MADEJSKI, Paweł; CHMIEL, Karolina; SUBRAMANIAN, Navaneethan; KUŚ, Tomasz. Methods and Techniques for CO2 Capture: Review of Potential Solutions and Applications in Modern Energy Technologies. en. **Energies**, v. 15, n. 3, p. 887, Jan. 2022. Number: 3 Publisher: Multidisciplinary Digital Publishing Institute. ISSN 1996-1073.

MALHOTRA, Deepika; CANTU, David C.; KOECH, Phillip K.; HELDEBRANT, David J.; KARKAMKAR, Abhijeet; ZHENG, Feng; BEARDEN, Mark D.; ROUSSEAU, Roger; GLEZAKOU, Vassiliki-Alexandra. Directed Hydrogen Bond Placement: Low Viscosity Amine Solvents for CO2 Capture. **ACS Sustainable Chem. Eng.**, v. 7, n. 8, p. 7535–7542, Apr. 2019. Publisher: American Chemical Society.

MATSUZAKI, Yoichi; YAMADA, Hidetaka; CHOWDHURY, Firoz A.; YAMAMOTO, Shin; GOTO, Kazuya. Ab Initio Study of CO2 Capture Mechanisms in Aqueous 2-Amino-2-methyl-1-propanol: Electronic and Steric Effects of Methyl Substituents on the Stability of Carbamate. **Ind. Eng. Chem. Res.**, v. 58, n. 8, p. 3549–3554, Feb. 2019. Publisher: American Chemical Society. ISSN 0888-5885.

MONTEIRO, Juliana G. M. -S.; SVENDSEN, Hallvard F. The N2O analogy in the CO2 capture context: Literature review and thermodynamic modelling considerations. **Chemical Engineering Science**, v. 126, p. 455–470, Apr. 2015. ISSN 0009-2509.

MORROW, Brian H.; HARRISON, Judith A. Vapor–Liquid Equilibrium Simulations of Hydrocarbons Using Molecular Dynamics with Long-Range Lennard-Jones Interactions. **Energy Fuels**, v. 33, n. 2, p. 848–858, Feb. 2019. ISSN 0887-0624.

N.BORHANI, Tohid; WANG, Meihong. Role of solvents in CO2 capture processes: The review of selection and design methods. **Renewable and Sustainable Energy Reviews**, v. 114, p. 109299, Oct. 2019. ISSN 1364-0321.

NOROOZI, Javad; SMITH, William R. Accurately Predicting CO2 Reactive Absorption Properties in Aqueous Alkanolamine Solutions by Molecular Simulation Requiring No Solvent Experimental Data. **Ind. Eng. Chem. Res.**, v. 59, n. 40, p. 18254–18268, Oct. 2020. Publisher: American Chemical Society. ISSN 0888-5885.

NOROOZI, Javad; SMITH, William R. Prediction of Alkanolamine pKa Values by Combined Molecular Dynamics Free Energy Simulations and ab Initio Calculations. **J. Chem. Eng. Data**, v. 65, n. 3, p. 1358–1368, Mar. 2020. Publisher: American Chemical Society. ISSN 0021-9568.

NÚÑEZ-ROJAS, Edgar; AGUILAR-PINEDA, Jorge Alberto; PÉREZ DE LA LUZ, Alexander; JESÚS GONZÁLEZ, Edith Nadir de; ALEJANDRE, José. Force Field Benchmark of the TraPPE_UA for Polar Liquids: Density, Heat of Vaporization, Dielectric Constant, Surface Tension, Volumetric Expansion Coefficient, and Isothermal Compressibility. **J. Phys. Chem. B**, v. 122, n. 5, p. 1669–1678, Feb. 2018. Publisher: American Chemical Society. ISSN 1520-6106.

ORLOV, Alexey A.; DEMENKO, Daryna Yu.; BIGNAUD, Charles; VALTZ, Alain; MARCOU, Gilles; HORVATH, Dragos; COQUELET, Christophe; VARNEK, Alexandre; MEYER, Frédérick de. Chemoinformatics-Driven Design of New Physical Solvents for Selective CO2 Absorption. **Environ. Sci. Technol.**, v. 55, n. 22, p. 15542–15553, Nov. 2021. Publisher: American Chemical Society. ISSN 0013-936X.

ORLOV, Alexey A. et al. Computational screening methodology identifies effective solvents for CO2 capture. en. **Commun Chem**, v. 5, n. 1, p. 1–7, Mar. 2022. Number: 1 Publisher: Nature Publishing Group. ISSN 2399-3669.

OROZCO, Gustavo A.; ECONOMOU, Ioannis G.; PANAGIOTOPOULOS, Athanassios Z. Optimization of Intermolecular Potential Parameters for the CO2/H2O Mixture. **J. Phys. Chem. B**, v. 118, n. 39, p. 11504–11511, Oct. 2014. Publisher: American Chemical Society. ISSN 1520-6106.

OROZCO, Gustavo A.; LACHET, Véronique; MACKIE, Allan D. Physical Absorption of Green House Gases in Amines: The Influence of Functionality, Structure, and

Cross-Interactions. **J. Phys. Chem. B**, v. 120, n. 51, p. 13136–13143, Dec. 2016. Publisher: American Chemical Society. ISSN 1520-6106.

OROZCO, Gustavo A.; LACHET, Véronique; NIETO-DRAGHI, Carlos; MACKIE, Allan D. A Transferable Force Field for Primary, Secondary, and Tertiary Alkanolamines. **J. Chem. Theory Comput.**, v. 9, n. 4, p. 2097–2103, Apr. 2013. Publisher: American Chemical Society. ISSN 1549-9618.

OROZCO, Gustavo A.; NIETO-DRAGHI, Carlos; MACKIE, Allan D.; LACHET, Véronique. Equilibrium and Transport Properties of Primary, Secondary and Tertiary Amines by Molecular Simulation. en. **Oil Gas Sci. Technol. – Rev. IFP Energies nouvelles**, v. 69, n. 5, p. 833–849, 2014. Number: 5 Publisher: Technip. ISSN 1294-4475, 1953-8189.

OROZCO, Gustavo A.; NIETO-DRAGHI, Carlos; MACKIE, Allan D.; LACHET, Véronique. Transferable Force Field for Equilibrium and Transport Properties in Linear and Branched Monofunctional and Multifunctional Amines. II. Secondary and Tertiary Amines. **J. Phys. Chem. B**, v. 116, n. 21, p. 6193–6202, May 2012. Publisher: American Chemical Society. ISSN 1520-6106.

OROZCO, Gustavo A.; NIETO-DRAGHI, Carlos; MACKIE, Allan D.; LACHET, Véronique. Transferable Force Field for Equilibrium and Transport Properties in Linear, Branched, and Bifunctional Amines I. Primary Amines. **J. Phys. Chem. B**, v. 115, n. 49, p. 14617–14625, Dec. 2011. Publisher: American Chemical Society. ISSN 1520-6106.

PAPADOPOULOS, Athanasios I.; ZAROGIANNIS, Theodoros; SEFERLIS, Panos. Computer-aided Molecular Design of CO2 Capture Solvents and Mixtures. In: PROCESS Systems and Materials for CO2 Capture. [S.l.]: John Wiley & Sons, Ltd, 2017. Section: 7 _eprint: https://onlinelibrary.wiley.com/doi/pdf/10.1002/9781119106418.ch7. P. 173–201. ISBN 978-1-119-10641-8.

PRAUSNITZS, Jhon M.; LICHTENTHALER, Rüdiger N.; GOMES DE AZEVEDO, Edmundo. **Molecular Thermodynamics of Fluid Phase Equilibria**. Third Edition. [S.l.]: Prentice Hall PTR.

RAINBOLT, James E.; KOECH, Phillip K.; YONKER, Clement R.; ZHENG, Feng; MAIN, Denise; WEAVER, Matt L.; LINEHAN, John C.; HELDEBRANT, David J.

Anhydrous tertiary alkanolamines as hybrid chemical and physical CO2 capture reagents with pressure-swing regeneration. en. **Energy Environ. Sci.**, v. 4, n. 2, p. 480–484, Feb. 2011. Publisher: The Royal Society of Chemistry. ISSN 1754-5706.

ROZANSKA, Xavier; WIMMER, Erich; MEYER, Frédérick de. Quantitative Kinetic Model of CO2 Absorption in Aqueous Tertiary Amine Solvents. **J. Chem. Inf. Model.**, v. 61, n. 4, p. 1814–1824, Apr. 2021. Publisher: American Chemical Society. ISSN 1549-9596.

SCHNABEL, Thorsten; VRABEC, Jadran; HASSE, Hans. Henry's law constants of methane, nitrogen, oxygen and carbon dioxide in ethanol from 273 to 498K: Prediction from molecular simulation. **Fluid Phase Equilibria**, v. 233, n. 2, p. 134–143, June 2005. ISSN 0378-3812.

SEN, Raktim; KOCH, Christopher J.; GOEPPERT, Alain; PRAKASH, G. K. Surya. Tertiary Amine-Ethylene Glycol Based Tandem CO2 Capture and Hydrogenation to Methanol: Direct Utilization of Post-Combustion CO2. en. **ChemSusChem**, v. 13, n. 23, p. 6318–6322, 2020. _eprint: https://onlinelibrary.wiley.com/doi/pdf/10.1002/cssc.202002285. ISSN 1864-564X.

SEVERIN, Kay. Synthetic chemistry with nitrous oxide. en. **Chem. Soc. Rev.**, v. 44, n. 17, p. 6375–6386, Aug. 2015. Publisher: The Royal Society of Chemistry. ISSN 1460-4744.

SHUKLA, Priyadarshi R. et al. Climate Change 2022: Mitigation of Climate Change. Contribution of Working Group III to the Sixth Assessment Report of the Intergovernmental Panel on Climate Change. en, 2022.

SKYLOGIANNI, Eirini; PERINU, Cristina; CERVANTES GAMEROS, Blanca Y.; KNUUTILA, Hanna K. Carbon dioxide solubility in mixtures of methyldiethanolamine with monoethylene glycol, monoethylene glycol–water, water and triethylene glycol. **The Journal of Chemical Thermodynamics**, v. 151, p. 106176, Dec. 2020. ISSN 0021-9614.

SKYNER, R. E.; MCDONAGH, J. L.; GROOM, C. R.; MOURIK, T. van; MITCHELL, J. B. O. A review of methods for the calculation of solution free energies and the modelling of systems in solution. en. **Phys. Chem. Chem. Phys.**, v. 17, n. 9, p. 6174–6191, Feb. 2015. Publisher: The Royal Society of Chemistry. ISSN 1463-9084.

SMITH, Kathryn H.; ASHKANANI, Husain E.; MORSI, Badie I.; SIEFERT, Nicholas S. Physical solvents and techno-economic analysis for pre-combustion CO2 capture: A review. **International Journal of Greenhouse Gas Control**, v. 118, p. 103694, July 2022. ISSN 1750-5836.

SONG, Zhen; SHI, Huaiwei; ZHANG, Xiang; ZHOU, Teng. Prediction of CO2 solubility in ionic liquids using machine learning methods. **Chemical Engineering Science**, v. 223, p. 115752, Sept. 2020. ISSN 0009-2509.

TOLLEY, W. K.; IZATT, R. M.; OSCARSON, J. L. Simultaneous measurement of excess enthalpies and solution densities in a flow calorimeter. **Thermochimica Acta**, v. 181, p. 127–141, May 1991. ISSN 0040-6031.

TOUTOUNI, Reihaneh; KUBELKA, Jan; PIRI, Mohammad. Liquid–Vapor Interfacial Tension in Alkane Mixtures: Improving Predictive Capabilities of Molecular Dynamics Simulations. **J. Phys. Chem. B**, v. 126, n. 5, p. 1136–1146, Feb. 2022. Publisher: American Chemical Society. ISSN 1520-6106.

UNGERER, Philippe; BEAUVAIS, Christèle; DELHOMMELLE, Jérôme; BOUTIN, Anne; ROUSSEAU, Bernard; FUCHS, Alain H. Optimization of the anisotropic united atoms intermolecular potential for *n* -alkanes. en. **The Journal of Chemical Physics**, v. 112, n. 12, p. 5499–5510, Mar. 2000. ISSN 0021-9606, 1089-7690.

VERSTEEG, Geert F.; VAN SWAAIJ, Wim P. M. Solubility and diffusivity of acid gases (carbon dioxide, nitrous oxide) in aqueous alkanolamine solutions. **J. Chem. Eng. Data**, v. 33, n. 1, p. 29–34, Jan. 1988. Publisher: American Chemical Society. ISSN 0021-9568.

WADE JR., Leroy G.; SIMEK, Jan William. **Organic Chemistry**. Ninth Edition. [S.l.]: Pearson.

WANDERLEY, Ricardo R.; PINTO, Diego D. D.; KNUUTILA, Hanna K. From hybrid solvents to water-lean solvents – A critical and historical review. **Separation and Purification Technology**, v. 260, p. 118193, Apr. 2021. ISSN 1383-5866.

WANG, Y. W.; XU, S.; OTTO, F. D.; MATHER, A. E. Solubility of N2O in alkanolamines and in mixed solvents. **The Chemical Engineering Journal**, v. 48, n. 1, p. 31–40, Jan. 1992. ISSN 0300-9467.

WORMALD, C. J; EYEARS, J. M. Excess molar enthalpies and excess molar volumes of {xCO2 + (1 x)C2H6} up to 308.4 K and 11.0 MPa. **The Journal of Chemical Thermodynamics**, v. 20, n. 3, p. 323–331, Mar. 1988. ISSN 0021-9614.

YANG, Xin; REES, Robert J.; CONWAY, William; PUXTY, Graeme; YANG, Qi; WINKLER, David A. Computational Modeling and Simulation of CO2 Capture by Aqueous Amines. **Chem. Rev.**, v. 117, n. 14, p. 9524–9593, July 2017. Publisher: American Chemical Society. ISSN 0009-2665.

YANG, Zequn; CHEN, Boshi; CHEN, Hongmei; LI, Hailong. A critical review on machine-learning-assisted screening and design of effective sorbents for carbon dioxide (CO2) capture. **Frontiers in Energy Research**, v. 10, 2023. ISSN 2296-598X.

YIANNOURAKOU, Marianna; UNGERER, Philippe; LEBLANC, Benoit; FERRANDO, Nicolas; TEULER, Jean-Marie. Overview of MedeA®-GIBBS capabilities for thermodynamic property calculation and VLE behaviour description of pure compounds and mixtures: application to polar compounds generated from ligno-cellulosic biomass. **Molecular Simulation**, v. 39, n. 14-15, p. 1165–1211, Dec. 2013. Publisher: Taylor & Francis _eprint: https://doi.org/10.1080/08927022.2013.830182. ISSN 0892-7022.

ZHANG, Wanxiang; WANG, Yan; REN, Shuhang; HOU, Yucui; WU, Weize. Novel Strategy of Machine Learning for Predicting Henry's Law Constants of CO2 in Ionic Liquids. **ACS Sustainable Chem. Eng.**, v. 11, n. 15, p. 6090–6099, Apr. 2023. Publisher: American Chemical Society.

ZHU, Aimei; ZHANG, Xinbo; LIU, Qinglin; ZHANG, Qiugen. A Fully Flexible Potential Model for Carbon Dioxide. **Chinese Journal of Chemical Engineering**, v. 17, n. 2, p. 268–272, Apr. 2009. ISSN 1004-9541.